

**SYNTHESIS AND STRUCTURAL INVESTIGATIONS OF
PYRIDINE-BASED AROMATIC FOLDAMERS**

FANG XIAO

(B.Sc.), SOOCHOW UNIVERSITY, CHINA

**A THESIS SUBMITTED
FOR THE DEGREE OF MASTER OF SCIENCE
DEPARTMENT OF CHEMISTRY
NATIONAL UNIVERSITY OF SINGAPORE**

Acknowledgements

It is a great pleasure to thank my supervisors, **Dr. Zeng Huaqiang, Ph. D.**, Assistant professor, Department of chemistry, National university of Singapore, for his invaluable guidance and advice throughout these years of my work. He has greatly devoted his valuable time to help me in this project and thesis, not only for sharing his knowledge but also encouragement and constant guidance.

I would like to express my sincere gratitude to all research staffs and postgraduate students in Dr. Zeng's group, especially to Ong Wei Qiang, Dr. Qin Bo, Liang Huifang, Yan Yan, Shu Yingying and Ren Changliang for their kind help, collaboration and friendship.

I would also like to express my gratitude to the Department of Chemistry and National University of Singapore for the award of the research scholarship.

Last but not least, I am very thankful to my family especially my parents and my friends for their warmest patience, moral support, great helps and encouragement for carrying out this project.

Thank you.

Fang Xiao

Table of Contents

Acknowledgements	i
Table of Contents	ii
Summary	v
List of Tables	vi
List of Figures	vii
List of Illustrations	x
Chapter One: Introduction	1
1.1 General.....	1
1.2 Cation-Conducting Channels.....	5
1.3 Anion-Conducting Channels	14
1.4 Applications of Ion Channels	15
References.....	17
Chapter Two: Synthesis and Structural Investigations of Pyridine-Based	
Aromatic Foldamers	20
2.1 Introduction.....	20
2.2 Theoretical Modeling.....	22
2.2.1 <i>Dimer</i>	23
2.2.2 <i>Trimer</i>	24
2.2.3 <i>Higher Acyclic Oligomers</i>	24

2.2.4 Cyclic Hexamer	29
2.2.5 Cyclic Pentamer	30
2.2.6 Cyclic Tetramer	31
2.3 Experimental Section	32
2.3.1 General Remarks	32
2.3.2 Synthetic Scheme	33
2.3.3 Synthetic Procedure	35
2.4 Results and Discussion	51
2.4.1 Synthesis of the Monomer and Higher Oligomers.....	51
2.4.2 X-Ray Crystal Structure Analysis	52
2.4.3 1D ¹ H NMR for Oligomers	53
2.4.4 2D NOESY Results	53
2.4.5 Variable Temperature ¹ H NMR Study on Pentamer 22	56
2.4.6 Binding Study by Dilution Method	57
2.5 Conclusion	61
References	62
Chapter Three: New Method for Demethylation of Aryl Methyl Ether	63
3.1 Introduction.....	63
3.2 Experimental	65
3.2.1 Synthetic Scheme	65

3.2.2 Synthetic Procedure	66
3.2.3 Procedure for Demethylation	69
3.3 Results and Discussion	70
3.3.1 Demethylation Using TBACl	70
3.3.2 Demethylation for Dimer	73
3.4 Conclusion	75
References.....	75
Chapter Four: Concluding Remarks	77

Summary

The primary aim of this thesis is to establish the folding patterns that may be seen in a series of pyridine-based crescent aromatic γ -peptides. By appending these conformationally defined cavity-enclosing oligomers to some linear scaffolds, a synthetic ion channel may be constructed, potentially forming an ion-conducting synthetic ion channel with tailored properties when embedded within the lipid bilayer membrane.

Both experimental approach and theoretical modeling were adopted to examine the design principles that underline the utilization of strong, directional multiply-centered hydrogen bonding interactions to restrict the rotational freedom of the aryl-amide bonds and enforce a crescent structure in a number of aromatic foldamers incorporating up to five monomeric, pyridine-based building blocks. The rigidified lengthened backbones were shown to enclose a sizable cavity decorated by amide protons and pyridine nitrogen atoms, which led us to believe that such amide protons-containing, cavity-enclosing oligomers may bind to various anions via hydrogen bonds formed between amide protons and anions. While results obtained from X-ray crystallography and 2D NOESY showed that the synthetic aromatic γ -peptides indeed adopt a crescent conformation with a desired cavity, dilution experiments indicated that these pyridine-based oligomers do not bind to the anions such as Cl^- , Br^- and I^- .

List of Tables

Table 2.1	Association Constants of Tetramer and Trimer with Iodide Anion.....	61
Table 3.1	Effects of Salts on the TBACl-Mediated Demethylation of Compound 2	72
Table 3.2	Effects of Salts on the TBACl-Mediated Demethylation of compound 5	72
Table 3.3	Effects of Solvents and Temperature on the TBACl-Mediated Demethylation of Compound 2	72

List of Figures

Figure 1.1	Classical Motifs Observed in Various Synthetic Ion Channel Model Systems	4
Figure 1.2	Kobuke's Synthetic Ion Channel	5
Figure 1.3	A Schematic Representation of Hypothetical Half Ion Channel with Cation Movement in the Channel	5
Figure 1.4	Kokube's Hypothetical Model of Resorcinol-Based Potassium-Selective Ion Channel	6
Figure 1.5	Modification of the K ⁺ -Selective Resorcinol-Based Ion Channel with Methyl Cholate	7
Figure 1.6	Gokel's Ion Channel Compound	7
Figure 1.7	Representation of Gokel's Channel	8
Figure 1.8	Covalently Bonded Macrotetracycle	8
Figure 1.9	Ferrocene-Based Ion Channel Compound	9
Figure 1.10	Schematic Depiction of the Cyclic Peptide Subunit	10
Figure 1.11	Gahadiri's Ion Channel Derived from Cyclic Peptide Nanotube	10
Figure 1.12	Ion Channel Compound	11
Figure 1.13	Formation of β -Barrel through β -Sheet Formation	12
Figure 1.14	Ligand-Gated Barrel-Stack Ion Channel	12
Figure 1.15	Structure of Bolaamphiphiles	13
Figure 1.16	Anion-Selective Cyclodextrin-Based Ion Channel	14
Figure 1.17	Chloride-Selective Ion Channel Involving Heptapeptide	15
Figure 2.1	Conceptual Depiction of the Synthetic Pore-Forming, Ion Conducting	

	Channel Embedded within A Phospholipid Bilayer Membrane.....	22
Figure 2.2	<i>Ab Initio</i> Results of Three Different Conformers of Dimer 2	26
Figure 2.3	<i>Ab Initio</i> Results of Three Different Conformers of Trimer 3	27
Figure 2.4	<i>Ab Initio</i> Calculation Results of Acyclic Trimer 3d , Tetramer 4a , Pentamer 5a , and Hexamer 6a	28
Figure 2.5	(a) Graphical Representation of Cyclic Hexamer 6b . (b) <i>Ab Initio</i> Calculated Structure of Cyclic Hexamer 6b	29
Figure 2.6	(a) Graphical Representation of Cyclic Pentamer 5b . (b) Axial View and (c) Side View of <i>Ab Initio</i> Calculated Structure of Cyclic Pentamer 5b	30
Figure 2.7	(a) Graphical Representation of Cyclic Tetramer 4b . (b) Axial View and (c) Side View of <i>ab Initio</i> Calculated Structure of Cyclic Tetramer 4b	31
Figure 2.8	X-Ray Structure of Dimer 2d	52
Figure 2.9	¹ H NMR of a) Dimer 16 , b) Trimer 18 , c) Tetramer 20 and d) Pentamer 22 in CDCl ₃	53
Figure 2.10	Structure of Dimer 23	53
Figure 2.11	2D NOESY Spectra of Dimer in CDCl ₃	54
Figure 2.12	(a) Structure, (b) and (c) 2D NOESY spectra of trimer 24 in CDCl ₃	55
Figure 2.13	¹ H NMR Spectra of Pentamer (22) in CDCl ₃ at (a) 303 K, (b) 293 K (c) 283 K and (d) 273 K.....	56
Figure 2.15	Nonlinear Regression Analysis of the Dilution Experiment Performed on 1:1 Complex of Chloride Ion with (a) Tetramer 20 and (b) Trimer 18	59
Figure 2.16	Nonlinear Regression Analysis of the Dilution Experiment Performed on 1:1 Complex of Bromide Ion with (a) Tetramer 20 and (b) Trimer 18	59

Figure 2.17	Nonlinear Regression Analysis of the Dilution Experiment Performed on 1:1 Complex of Iodide Ion with (a) Tetramer 20 and (b) Trimer 18	60
Figure 3.1	1D NOE of Dimer 6	73

List of Abbreviations

CDCl ₃	Deuterated Chloroform
DCM	Dichloromethane
DMF	Dimethylformamide
DMSO	Dimethyl sulfoxide
DMSO-d ₆	Deuterated Dimethyl Sulfoxide
EA	Ethyl Acetate
MeOH	Methanol
NMP	<i>N</i> -methyl-2-pyrrolidone
NMR	Nuclear Magnetic Resonance
Pd/C	Palladium on Carbon
THF	Tetrahydrofuran
1D	1-Dimensional
2D	2-Dimensional
TBA	Tetrabutylammonium

Chapter One

Introduction

1.1 General

Nature's way of folding biopolymers into different tertiary and quaternary structures has led to the development of many different astonishingly efficient and sophisticated ion channels.¹ Naturally occurring ion channels are large protein ensembles encompassing (1) a central channel portion that spans the phospholipid bilayer membranes (25 Å to 50 Å in thickness) and (2) an additional region on either or both side of the channel to control accessibility into the channel portion.² They function as transport devices for inorganic ions across the membranes and show unparalleled conduction rates and selectivity for specific ions. In certain cases, unidirectional conduction of ions can also be achieved.³ The transportation of molecules across the lipid bilayer membranes is mediated by pores.⁴

The selective and regulated transportation of ions and molecules between intra- and extra-cellular components of the cell is the primary role of the protein-based ion channels. Transportation or translocation of molecules and ions across the lipid bilayer membrane occur via two different mechanisms, namely the carrier mechanism and the channel transport mechanism.⁵ The former involves the encapsulation and transportation of the molecule or ion across the lipid bilayer membrane by a membrane soluble entity. The latter involves a pore spanning the

membrane which would allow the molecule or ion to flow through it to the other side of the membrane. It was believed that at the earlier stages of evolution, simpler “primordial channels”, which are not as efficient and selective as their modern counterpart, were in operation. Natural selection and adaptation during evolution has eventually led to the formation of these ion channels with advantageous traits. Consequently, many research groups have devoted intensive efforts into the development and construction of folding oligomers and polymers into well defined nanoscale supramolecular structures which may have protein-like functions.⁶⁻¹⁰

Numerous artificial (also known as synthetic) ion channels have been synthesized by different groups and they can be broadly categorized into several groups, namely peptidic or non-peptidic; α -helical or β -barrels structures, with cationic or anionic interiors; ohmic and non-ohmic and so on. By definition, synthetic ion channels are compounds that have abiotic scaffolds and act in lipid bilayer membrane.¹¹ However, this definition does not apply to ion channels formed by natural products, bioengineered or chemically modified membrane proteins and peptides or *de novo* peptides.⁴

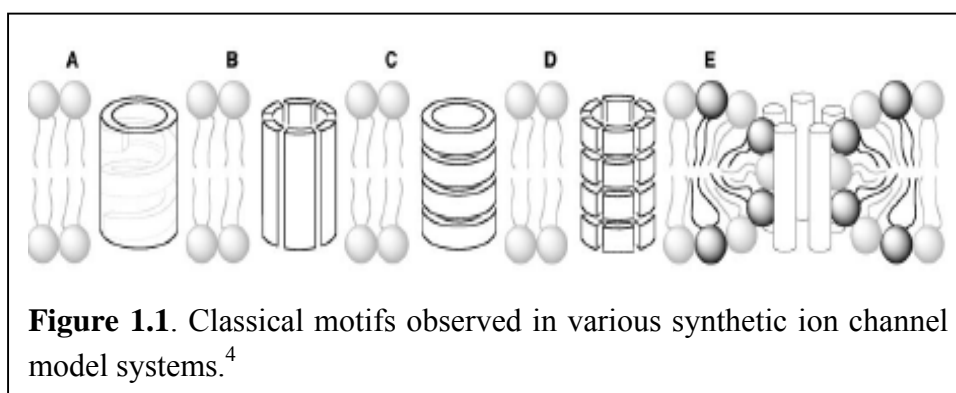
There are several important characteristics of synthetic ion channels, which include its size, pH, voltage, anion/cation selectivity, membrane selectivity, ligand gating and blockage. Synthetic ion channel should span the entire thickness of the lipid bilayer membrane. On top of that, the building blocks that make up the artificial

ion channel should contain both hydrophilic and hydrophobic groups to be stabilized in the biological environment. Ideally, the artificial ion channel should provide tunability of the cavity size and its interior properties, such as ion-binding capacity and interior hydrophobicity.

There are several techniques available for the characterization of the synthetic ion channel.² Common methods include planar lipid bilayer conductance experiment, ²³Na Nuclear Magnetic Resonance (NMR) translocation assay, fluorescence translocation assay, circular dichroism spectroscopy, infrared spectroscopy, 2-Dimensional (2D) NMR, size exclusion experiments and pH stat method.⁴ The planar lipid bilayer conductance experiment consists of a solution of the phospholipids membrane molecules in a Teflon plate separating two chambers. The phospholipids molecules will organize into the bilayer around a hole of typical 100 Å in diameter through which the conductance of the ions can be determined. ²³Na NMR spectroscopy is performed by adding a shift reagent such as Dy (III) to the extra-vesicular solution. The sodium nuclei outside the liposomes will thus have different chemical shifts as compare to the sodium nuclei inside the liposomes. UV/Vis or fluorescence spectroscopy can be used in situations in which there is a change in the chromophoric property of the molecule when complexed to the influxing metal ion used in the study inside the liposomes. Size exclusion experiments can be used to determine the inner diameter of the ion channel. pH stat method measures the efflux

of the protons from inside the liposomes to outside that is caused by a sudden increase of pH outside the liposomes. The efflux of the protons leads to measurable influx of metal cations into liposomes if the synthetic ion channels being studied indeed can all the metal ions to pass through.

Similarly, there are two different approaches to synthesize artificial ion channels: self-assembling from (1) multiple building blocks; (2) a single molecule. The synthesized artificial ion channels are classified into different categories based on their structures. The motifs often observed in synthetic ion channels include unimolecular macromolecules, complex barrel-stave, barrel-rosette, barrel hoop and micellar supramolecules (**Figure 1.1**).⁴

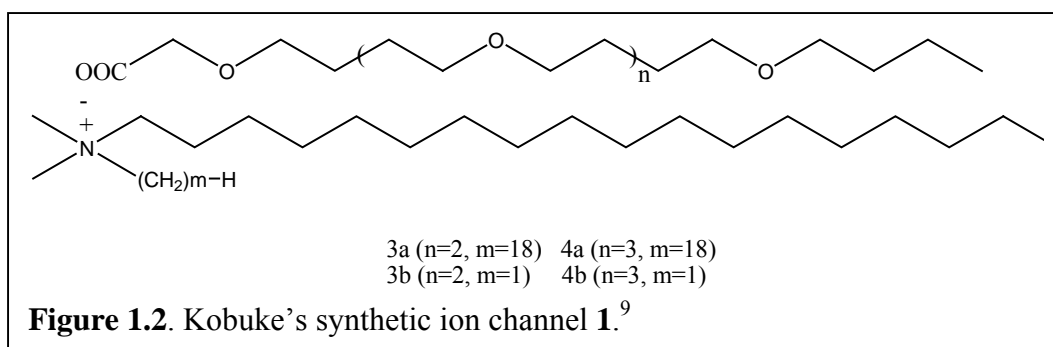


Although there are large amount of biochemical and cellular information available with regards to natural ion channel, to model and synthesize a synthetic ion channel system that can mimic the physiological function of its natural counterpart remains a difficult task. It is a goal pursued by many biologists and chemists in the

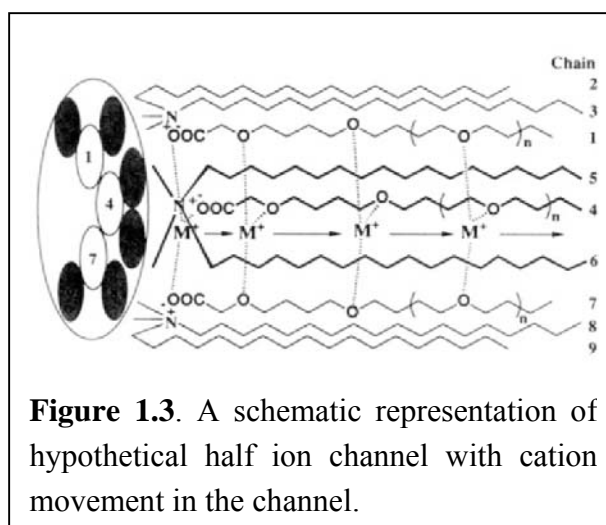
effort to synthesize an artificial ion channel system with tailored properties that mimic the biological function.

1.2 Cation-Conducting Channels

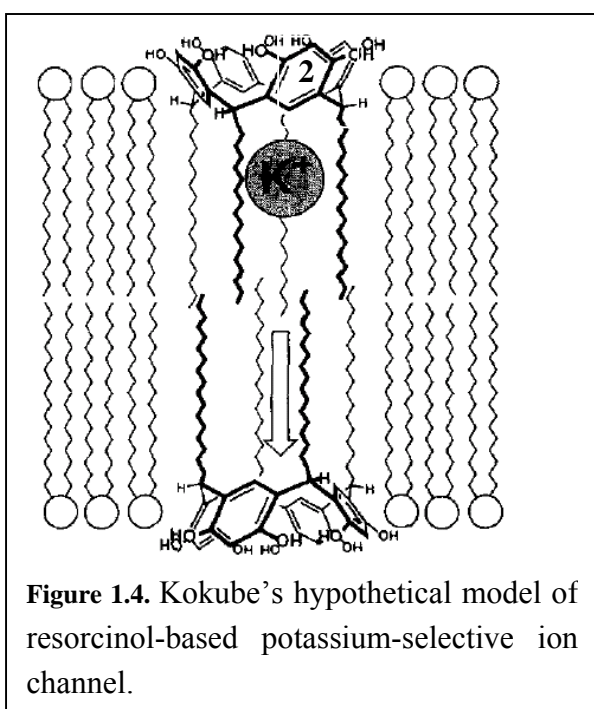
The first non-peptidic artificial ion channel was reported by Kobuke et al. in 1992.⁹ The channel **1** consisted of an amphiphilic ion pair made up of oligoether-carboxylates and mono- or di-octadecylammonium cations (**Figure 1.2**). The carboxylates formed the channel core while the cations formed the hydrophobic outer wall which was embedded in the bilipid membrane with a channel length of about 24 to 30 Å. The resultant ion channel, formed from molecular self-assembly, is cation selective and voltage dependent.



From the experimental results obtained, the above structure shown in **Figure 1.3** was proposed. The non-shaded circles 1, 4 and 7 represented the

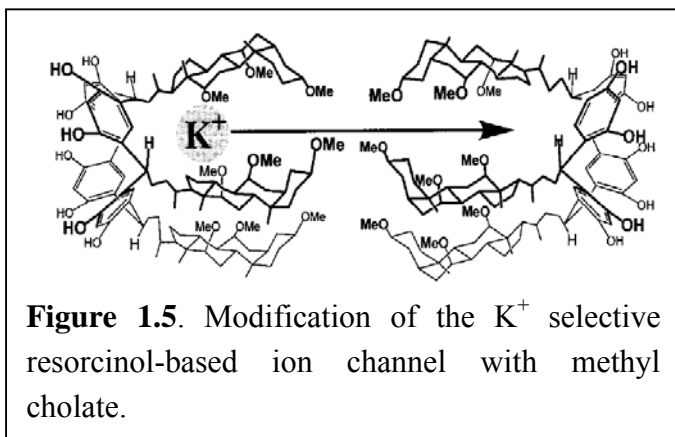


chains of oligoether-carboxylates which self-assembled to form the inner polar surface of the synthetic ion channel. Alternatively, the shaded circles represented the hydrophobic, alkyl chains of the octadecylammonium component which formed the hydrophobic wall of the ion channel. Metal cations represented by M^+ in the diagram can then pass through the membrane and are stabilized by coordination to the ether oxygen on their way through the hydrophobic membrane region. Experimental results had shown that the cation selectivity of the channel was due to the properties of the inner membrane structure but not the opening of the channel.¹²



A few years later, Kokube et al. synthesized another channel comprising of resorcinol-based cyclic tetramer **2** as the building block.¹³ The resorcin-[4]-arene monomer consisted of four long alkyl chains which aggregated to form a dimeric supramolecular structure resembling that of Gramicidin A (**Figure 1.4**).

The role of the long alkyl chain used was to prevent the lipid molecule from entering the channel and the formation of the dimer structure was preferred to prevent the bulky amphiphile from flip flopping around. The cavity of the tetramer was designed

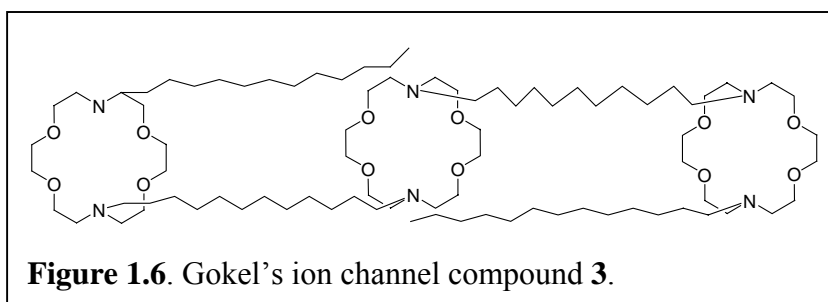


to allow the entry of potassium cation and experimental results showed that the channel was able to discriminate potassium ion from sodium ion.

Modification of the alkyl tail

with methyl cholate gave a long-lasting open state life time in the ion channel without affecting the cation selectivity (**Figure 1.5**).¹⁴

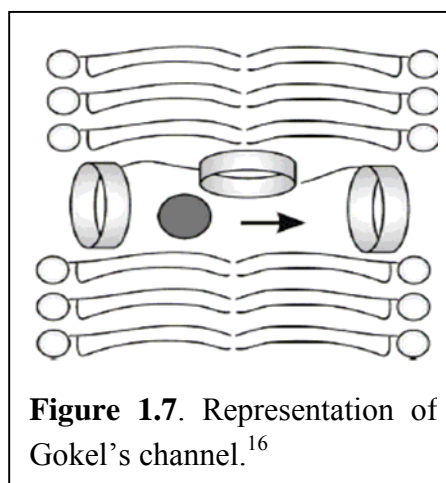
Crown ethers are common building blocks that have been



extensively used in constructing unimolecular ion channels.¹⁵ Gokel et al. had studied a simple yet fully functional ion channels, which known as “hydraphiles”.¹⁶ The model took on the general structure of “sidearm-crown-spacer-crown-spacer-crown-sidearm” and used crown ether as the head group as it was thought to be able to anchor the whole channel in an extended conformation in the lipid bilayer and yet capable of transporting cations through the channel. An example (channel **3**) is shown in **Figure 1.6**, consisting of diaza-18-crown-6 crown ether groups and alkyl chain as sidearms and spacers. Channel **3** is capable of transporting protons across the bilayer

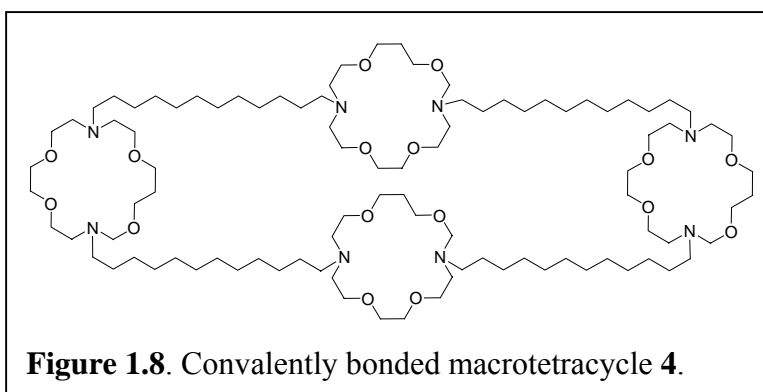
membrane. The central macrocycle serve as a central relay unit and helps to increase the cation flux through the channel. When the poly(ethylene oxide) sidearms were replaced by polymethylene chains, the proton flux increased due to a lack of oxygen donor atoms on the polymethylene chains. The oxygen atoms bind strongly with the protons which slowed their translocation across the channel.

Further works had shown that the central crown ether is essential for high activity; however, structural variants with smaller crown showed high activity as well and thus it is unlikely that cations passed through the central crown.¹⁶ High activity was



also observed when the central crown ether was replaced with $O(CH_2CHO)_3$ chains.¹⁷

These results indicated



that the active structure had its central macrocycle in a parallel conformation to the axis of the lipid bilayer (**Figure 1.7**). Experimental results had confirmed the conformation of the active structure. As mentioned, the central macrocycle is essential for high activity. A covalently bonded macrocycle 4 (**Figure 1.8**) had

shown to be about three times more active than **3** and its amide-containing analogue of **4** also showed enhanced activity.¹⁸

Not only can hydrophiles be synthesized easily, the width of the channel can also be easily tuned by using different length of alkyl groups so as to match the length of the lipid bilayer membrane.¹⁹ And as a result, many studies had been done on hydrophiles including electrophysiological studies on living cells.²⁰

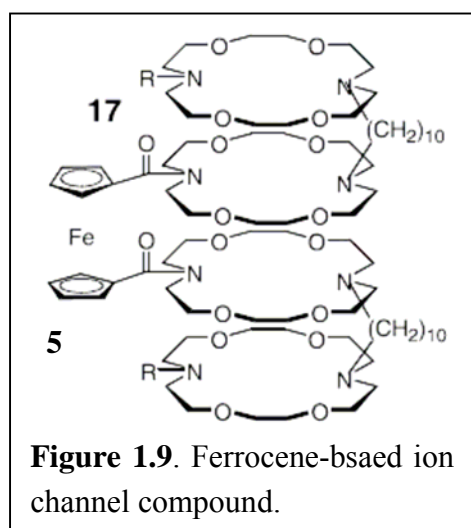


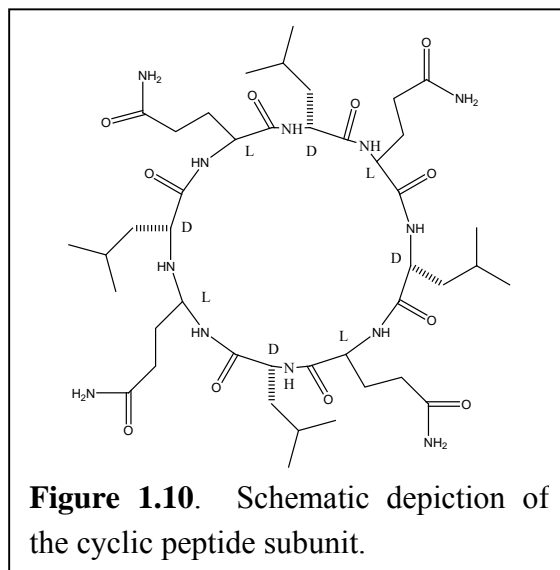
Figure 1.9. Ferrocene-based ion channel compound.

Besides using organic moiety to build synthetic ion channel, inorganic derivative using crown ethers had also been synthesized. Hall and its co-workers had synthesized an ion channel **5** using a ferrocene and 4 diaza-18-crown-6 linked by 2 dodecyl chains (**Figure 1.9**).²¹ The ion channel was redox-active as

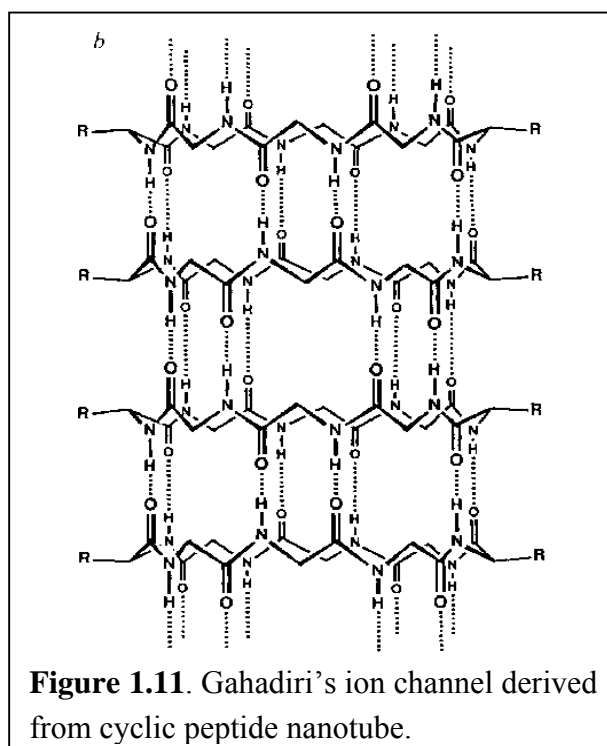
oxidation of the ferrocene caused the compound to switch to an inactive form.

All the channels described above belong to a class of tubular channel with classical unimolecular or monomeric motifs. Another class of tubular channel is the β -barrel. They are more difficult to synthesize as the channel formation usually involves self-assembly via non-covalent interactions.

A cyclic peptide composed of even number of alternating D- and L-amino acids (**Figure 1.10**) was suggested to form barrel-hoop structure through backbone-backbone hydrogen bonds by De Santis.¹⁰



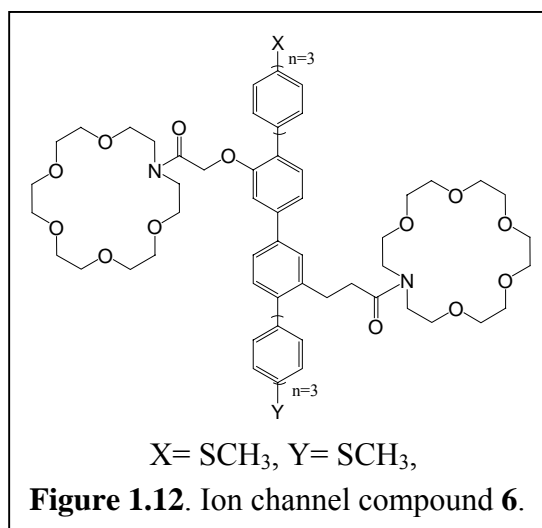
A tubular nanotube synthesized by Ghadiri et al. consisting of cyclic D and L peptide subunits was shown to adopt a flat, ring-shaped conformation that stack through an extensive anti-parallel β -sheet-like hydrogen bonding interaction (**Figure 1.11**).²² The alternating arrangement cause the side chains of the amino acids to be pointed



outwards from the channel, thus allowing an unobstructed passage for ions through the channel pores. As the channel was formed from self-assembly, one can tune the outer surface and diameter of the channel by using different types and/or number of amino acids. Experimental results had shown that the channel can transport sodium

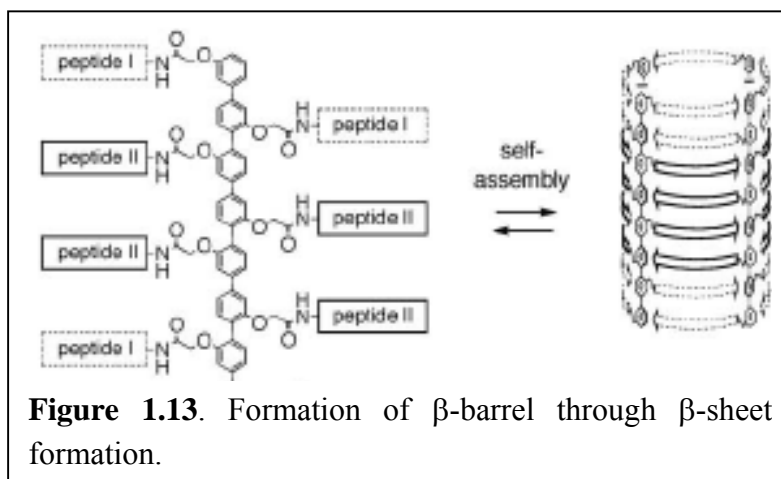
and potassium ions. The channel can also be constructed by the use of direct covalent bonding between the sheets so as to increase the thermodynamic and kinetic stability.²³ Therapeutic applications had been found with these nanotubes. Biocidal activity towards Bacteria Methicillin-Resistant *Staphylococcus aureus* (MRSA), Biofouling Algae *Ulva linza*, *E. coli* and *Navicula perminuta* had been found with a cyclic D,L-peptide hexamer synthesized.²⁴

As mentioned earlier, crown ethers are the most popular macrocycles used. Attaching pendant crown ethers to an octiphenyl scaffold lead to the formation of compound **6** (**Figure 1.12**). The advantage of using the scaffold is that it can control the

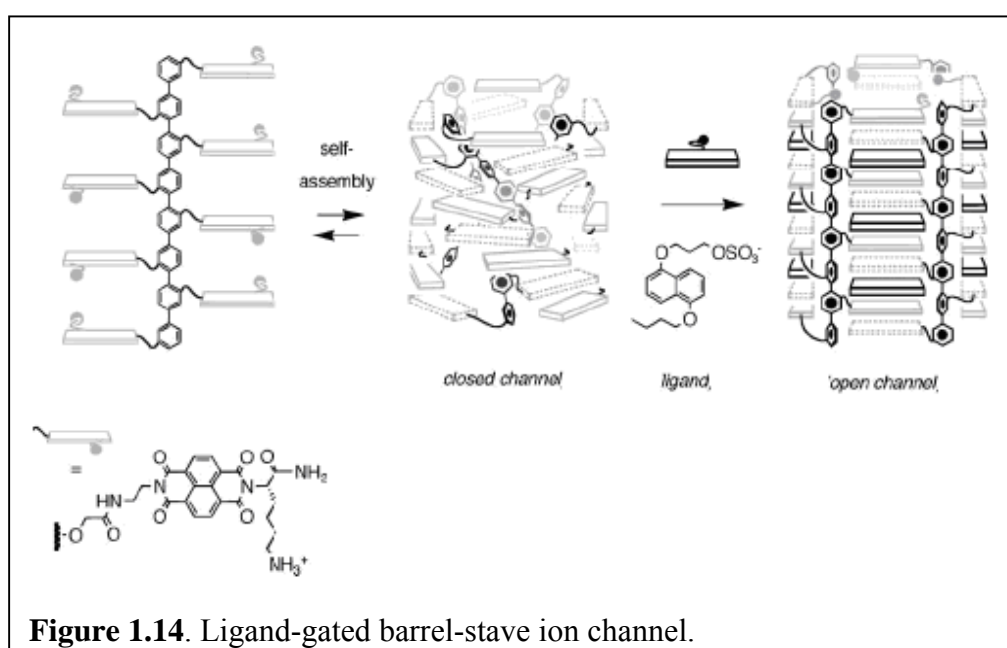


length and linearity of the structure. However the rotation and the face to face position of the crown ether are uncontrolled and are determined by non-covalent interactions. The ion channel is shown to be ineffective when both X and Y groups on **6** are neutral.¹¹

By attaching peptides to the octiphenyl scaffold, a β -barrel can be formed from self-assembly through the

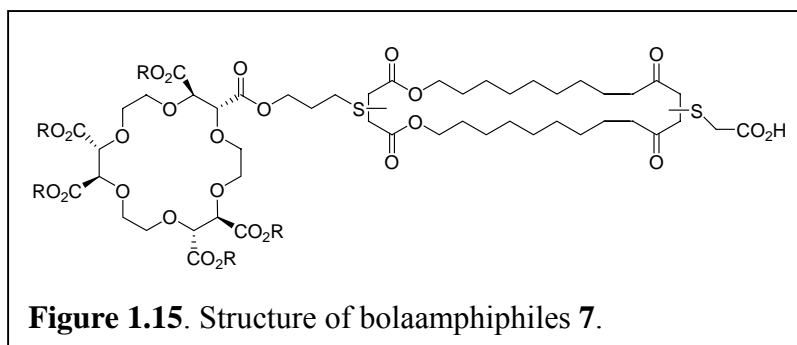


formation of β -sheet structures between the peptide chains (**Figure 1.13**). The formation of the β -sheet caused the side chain of the amino acids to point outwards thus creating a favorable environment for ion transportation as the exterior of the channel is hydrophobic and the interior is hydrophilic as it is water filled. The same scaffold was used by Matile et al. to mimic the structure of macrolide antibiotic amphotericin B.²⁵ The channel synthesized was shown to transport cations across the membrane.



One of the challenges in the field is to create an ion channel that will only open (ligand gating) or close (blockage) in response to chemical stimulation. Attaching the electron-poor naphthalenediimide (NDIs) to the same octiphenyl scaffold led to the hoop-stave mismatch during self-assembly that results in a twisted and closed channel conformation (**Figure 1.14**).²⁶ Adding the complementary dialkoxynaphthalene (DAN) donor led to the cooperative interactions between NDI and DAN that favors the formation of barrel-stave ion channel. The resultant anion-conducting ion channel was shown to be homogenous, ohmic and have low conductance.

Another motif observed in ion channel is the micellar motif. These aggregate



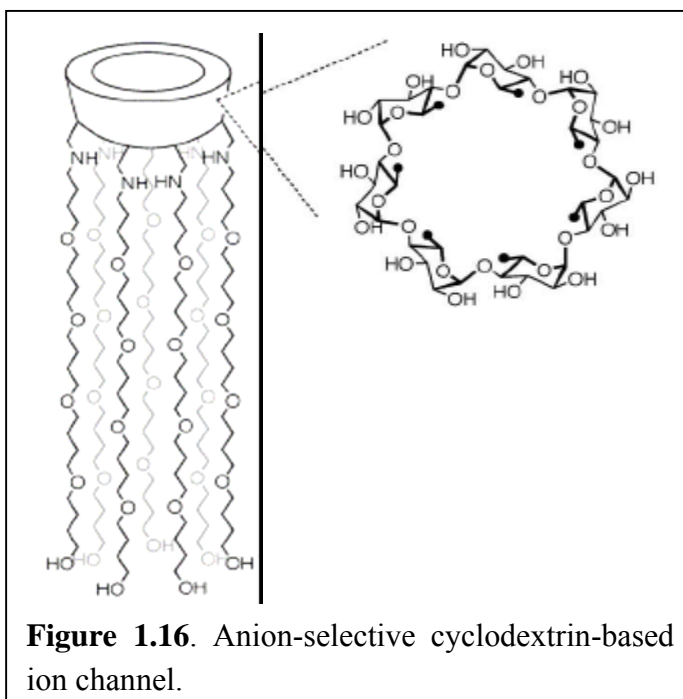
channels are formed by amphotericin involving both sterols and antibiotics arranged in two half-channel sections within the membrane.² This motif is uncommon in synthetic ion channel as it is very difficult to design these compounds which had to self-assemble together to form an ion channel. An active form of the compound is the bolaamphiphiles (two-headed amphiphiles). One such example is manifested by **7** (**Figure 1.15**) that forms an active channel structure through dimerization or

trimerization within the bilayer membrane. Electrochemical studies had shown that the monomer is inactive and the active form involves dimer or larger aggregates.

1.3 Anion-Conducting Channels

The artificial ion channels discussed so far are mostly cation-conducting. There had been very few example of anion conducting ion channel.²⁷⁻²⁹

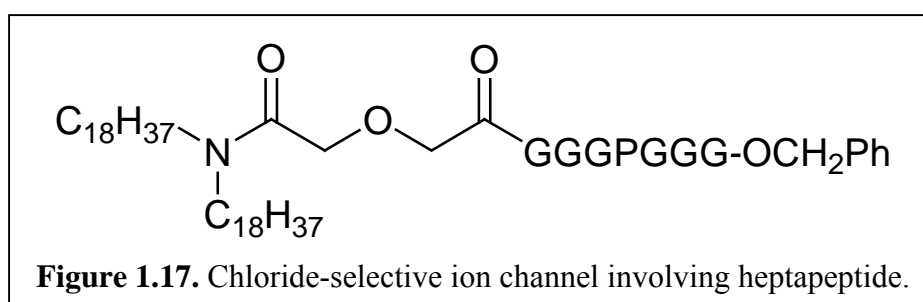
Several factors have to be considered when designing anion conducting ion



channels namely, the anion's shape, size and polarizability, pH dependence and its solvation. A highly active, anion selective, monomeric cyclodextrin-based ion channel was designed by Madhavan et al (**Figure 1.16**).²⁹ Oligoether chains were attached to the primary face of the β -cyclodextrin head group via amide bonds. The hydrophobic oligoether chains were chosen because they are long enough to span the entire lipid bilayer. Besides selecting anions over cations, the channel was also able to discriminate among halide anions in the order $I^- > Br^- > Cl^-$ (following Hofmeister

series). The anion selectivity came about with the ring of ammonium cations being positioned just beside the cyclodextrin head group which helped to select for anions. Iodide ion being the most polarizable was transported the fastest as the activation barrier to enter the hydrophobic channel core is lower for I^- compared to either Br^- or Cl^- .

A more specific artificial anion selective ion channel was the chloride selective ion channel synthesized by Gokel.³⁰ The building block involved a heptapeptide with Proline incorporated (**Figure 1.17**). Proline was found to be of importance within the chloride entry portal. The hydrophobic tail, which was designed based on mimicry of the phospholipids tails, anchored the heptapeptide in the top of the mid polar region of the lipid bilayer forming an uncharged, chloride selective portal.



1.4 Applications of Ion Channels:

Some demonstrated applications involving synthetic ion channels include nanoreactors for catalysis and chemical or biological sensors. They may also promise

some good interdisciplinary uses as nanofiltration membrane, drug or gene delivery vehicles/transporters as well as channel-based antibiotics that may kill bacterial cells preferentially over mammalian cells.

The aim of this project is to design and synthesize a new class of folding oligomers derived by linking pyridine rings via amide linkages. A synthetic ion channel may be obtained by appending these conformationally well defined cavity-enclosing oligomers to some linear scaffolds. Hopefully, this design could potentially form ion-conducting channels with tailored properties and ultimately lead to novel therapeutic agents in the future.

References

1. Gong, B.; Zeng, H.; Zhu, J.; Yuan, L.; Han, Y.; Cheng, S.; Furukawa, M.; Parra, R. D.; Kovalevsky, A. Y.; Mills, J. L.; Skrzypeczak-Jankun, E.; Martinovic, S.; Smith, R. D.; Zheng, C.; Szyperski, T.; Zeng, X. C. *Proc. Natl. Acad. Sci. USA* **2002**, 99, 11583.
2. Fyles, T. M. *Chem. Soc. Rev.* **2007**, 36, 335.
3. Schlesinger, P. H.; Ferdani, R.; Liu, J.; Pajewska, J.; Pajewski, R.; Saito, M.; Shabany, H.; Gokel, G. W. *J. Am. Chem. Soc.* **2002**, 124, 1848.
4. Sisson, A. L.; Shah, M. R.; Bhosale, S.; Matile, S. *Chem. Soc. Rev.* **2006**, 35, 1269.
5. Kotch, F. W. "Artificial Ion Channels" Available at http://organicdivision.org/essays_2001/kotch.pdf.
6. Gellman, S. H. *Acc. Chem. Res.* **1998**, 31, 173.
7. Rowan, A. E.; Nolte, R. J. M. *Angew. Chem.* **1998**, 37, 63.
8. Hill, D. J.; Mio, M. J.; Prince, R. B.; Hughes, T. S.; Moore, J. S. *Chem. Rev.* **2001**, 101, 3893.
9. Kobuke, Y.; Ueda, K.; Sokabe, M. *J. Am. Chem. Soc.* **1992**, 114, 7618.
10. De Santis, P.; Morosetti, S.; Rizzo, R. *Macromol.* **1974**, 7, 53.
11. Matile, S.; Som, A.; Sordé, N. *Tetrahedron*, **2004**, 60, 6405.
12. Kobuke, Y.; Morita, K. *Inorg. Chimica Acta* **1998**, 283, 167.

13. Yasutaka Tanaka, Y. K. M. S. *Angew. Chem. Int. Ed.* **1995**, 34, 693.
14. Naomi Yoshino, A. S. Y. K. *Angew. Chem. Int. Ed.* **2001**, 40, 457.
15. McNally, B. A.; Leevy, W. M.; Smith, B. D. *Supramol. Chem.* **2007**, 19, 29.
16. Murillo, O.; Watanabe, S.; Nakano, A.; Gokel, G. W. *J. Am. Chem. Soc.* **1995**, 117, 7665.
17. Gokel, G. W. *Chem. Commun.* **2000**, 1
18. Shabany, H.; Gokel, G. W. *Chem. Commun.* **2000**, 2373.
19. Leevy, W. M.; Weber, M. E.; Schlesinger, P. H.; Gokel, G. W. *Chem. Commun.* **2005**, 89.
20. Leevy, W. M.; Huettner, J. E.; Pajewski, R.; Schlesinger, P. H.; Gokel, G. W. *J. Am. Chem. Soc.* **2004**, 126, 15747.
21. Hall, A. C.; Suarez, C.; Hom-Choudhury, A.; Manu, A. N. A.; Hall, C. D.; Kirkovits, G. J.; Ghiriviga, I. *Org. Biomol. Chem.* **2003**, 1, 2973.
22. Ghadiri, M. R.; Granja, J. R.; Milligan, R. A. ; McRee, D. E. ; Khazanovich, N. *Nature* **1993**, 366, 324.
23. Clark, T. D.; Kobayashi, K.; Ghadiri, M. R. *Chemistry - A European Journal* **1999**, 5, 782.
24. Fletcher, J. T.; Finlay, J. A.; Callow, M. E.; Callow, J. A.; Ghadiri, M. R. *Chem. Eur. J.* **2007**, 13, 4008.

25. Sakai, N.; Brennan, K. C.; Weiss, L.; Matile, S. *J. Am. Chem. Soc.* **1997**, 119, 8726.
26. Talukdar, P.; Bollot, G.; Mareda, J.; Sakai, N.; Matile, S. *J. Am. Chem. Soc.*, **2005**, 127, 6528.
27. Gokel, G. W.; Mukhopadhyay, A. *Chem. Soc. Rev.* **2001**, 30, 274.
28. Koert, U.; Al-Momani, L. A.; Pfeifer, J. R. *Synthesis* **2004**, 8, 1129.
29. Madhavan, N.; Robert, E. C.; Gin, M. S. *Angew. Chem.* **2005**, 44, 1.
30. Schlesinger, P. H.; Ferdani, R.; Liu, J.; Pajewska, J.; Pajewski, R.; Saito, M.; Shabany, H.; Gokel, G. W. *J. Am. Chem. Soc.* **2002**, 124, 1848.

Chapter Two

Synthesis and Structural Investigations of Pyridine-Based Aromatic Foldamers

2.1 Introduction

As mentioned earlier in Chapter 1, there are not many supramolecular structures designed to conduct anions due to some intrinsic properties of anions and difficulties in designing hydrogen bond donors into the channel structure. Designing and developing an efficient anion transporter had been an emerging field. Chloride, bicarbonate, carbonate and phosphate are the few anions that are present and play very important biochemical or metabolic roles.¹ The distribution of these anions in various cells and tissues in the body are not even. The concentration gradients of these anions between the intracellular and extracellular fluids are created and maintained by ion channels embedded in the lipid bilayer membranes. Anions-conducting ion channels may not only shed some insights into the role and function of natural ion channels but also serve as useful tools for the studies of biochemistry, biophysics and physiology of natural ion channels, membrane transportation and medical application of these synthetic anion ion channels.

The first successful synthetic anion channel was designed by Tomich's group in the early 1990s using a short protein segment with the following sequence, HNPro-Ala-Arg-Val-Gly-Leu-Gly-Ile-Thr-Thr-Val-Leu-Thr-Met-Thr-Thr-Gln-Ser-Ser-Gly-

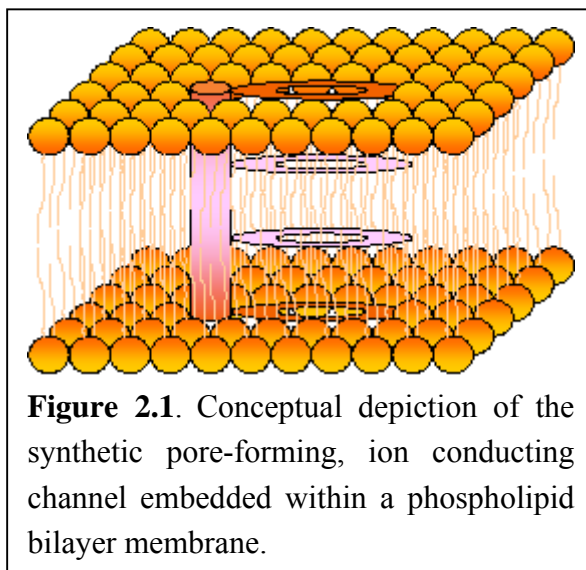
Ser-Arg-Ala.²⁻³ This sequence was adopted from a protein that lined the wall of a natural anion channel of the spinal cord glycine receptor. Tetrameric and pentameric aggregates of the synthesized peptide were shown to have channel activity and was found to be 85 % anion selective in potassium chloride solution. It was observed that by replacing the positively-charged arginines at the end of the peptide with glutamates, the channel became cation-selective.⁴ Peptides of other sequences had been synthesized and tested, and one of them had shown very high anion selectivity. Other examples of synthetic anionic channels had been discussed earlier in Chapter 1.

Studies had shown that the selectivity of anions by the natural ion channel proteins was achieved by having hydrogen bonding donors on the filter section of the proteins which can displace the solvated water molecules surrounding the anions and thus promoting anion transportation.¹ This chapter is focused on the design principles, theoretical calculation, synthetic and structural analysis of the pyridine-based crescent aromatic foldamers that may potentially bind to anions and possibly cations too.

Foldamers are synthetic oligomers with well-defined conformations enforced by non-covalent bonds.⁵⁻⁶ Recently, there had been an increasing interest on designing foldamers using unnatural building blocks that can adopt well-defined structure.⁵⁻⁹ Our approach made use of a convergent synthetic route to synthesize the crescent aromatic γ -peptides from a pyridine-based building block. The building block was designed in such a way that there would be directional intramolecular hydrogen

bonding present within the molecule.

The rigidification of the amide backbone conferred by the multiple-centre hydrogen bonding system would help to stabilize the formation of a well-defined crescent structure with its interior cavity decorated by



amide protons and pyridine nitrogen atoms. Our hypothesis is that the pyridine-based crescent aromatic γ -peptide would form hydrogen bonds to anions through its amide protons. On top of that, by varying the number of building blocks in the aromatic foldamers, the size of the interior cavity can be adjusted, leading to a good tunability in the ion-binding capacity of the resulting foldamers. Tunability of the foldamers' interior properties can be achieved further by incorporating different types of building blocks into the foldamers. Furthermore, we conceptualized the idea of appending circular γ -peptide to a linear scaffold that is rigidified by directional H-bonding interactions as shown in **Figure 2.1**.

2.2 Theoretical Calculation

Ab initio calculations were first performed on the designed aromatic γ -peptides using computational software Gaussian 98 (B3LYP/6-31G) to see if the molecules are planar and adopt a crescent conformation.

As mentioned earlier in the introduction, the design of the circular aromatic γ -peptides is based on amino acid residues with aromatic backbone and hence theoretical calculations were performed to determine the presence and the strength of intramolecular hydrogen bonding between the hydrogen bond donor and hydrogen bond acceptor. Due to the delocalization of the lone pair electrons on nitrogen into the C-N bond, the C-N bond assumes a partial double bond characteristic. This means that the C-N bond cannot rotate freely unless at elevated temperature. Nevertheless, the adjacent C-C bond and C-N bond could be rotated. Such rotations are suppressed by introducing intramolecular hydrogen-bonding forces.

2.2.1 Dimer

Theoretical calculations for three possible conformers of dimer were performed and the results were summarized in **Figure 2.2**.

The comparison in the relative energies involving these three conformers showed that conformers **2b** and **2c** are energetically less stable than conformer **2a** by 12.3 Kcal/mol and 8.3 Kcal/mol, respectively. This energy difference can be attributed to the number of stabilizing hydrogen bonding interactions present in these

three conformers. While the most stable conformer **2a** has 4 hydrogen bonds that form a three-center hydrogen bonding system, the conformers **2b** and **2c** have two and three hydrogen bonds, respectively. The presence of more hydrogen bonding forces in **2a** contributes to the higher stability in **2a** observed theoretically. All the calculated hydrogen bond distances in Angstrom (\AA) are in good agreement with typical hydrogen-bonding distances of 1.8 – 2.6 \AA . These modeling results suggest that experimental observation of the planar crescent structure in **1** is highly likely in the presence of some localized hydrogen bonds.

2.2.2 Trimer

The molecular modeling mentioned above was similarly applied to different conformers of trimer **3** (**Figure 2.3**). Just like the dimer **2**, the conformer **3c** having the most number of intramolecular hydrogen bonds (5 of them) is the most stable one and should adopt the crescent conformation. The relative energies of conformer **3a** (3 hydrogen bonds) and **3b** (4 hydrogen bonds) of trimer with respect to conformer **3c** are summarized in **Figure 2.3**.

2.2.3 Higher Acyclic Oligomers

Encouraged by the positive results obtained in the *ab initio* calculations for dimer and trimer, theoretical calculations were then performed on higher acyclic

oligomers (i.e. trimer **3d**, tetramer **4**, pentamer **5**, and hexamer **6**) to determine the number of residues per turn in their respective helical structures. This knowledge will then be utilized to guide our design of planar circular peptides. Such a desired planarity is critically important in our ion channel approach.

In agreement to what was proposed, *ab initio* results (**Figure 2.4**) showed that the trimer **3d**, acyclic tetramer **4a**, acyclic pentamer **5a** and acyclic hexamer **6a** did adopt a turn-like crescent structure with both tetramer **4a** and pentamer **5a** adopting a helical structure. The calculated structures from tetramer **4a** to hexamer **6a** shows a helical periodicity of about four residues per turn, suggesting that a head-to-tail cyclized circular tetramer adopt a planar circular conformation. *Ab initio* calculations were then performed on cyclic tetramer **4b** to test this hypothesis theoretically. For comparison, calculations on cyclic pentamer **5b** and hexamer **6b** were also performed.

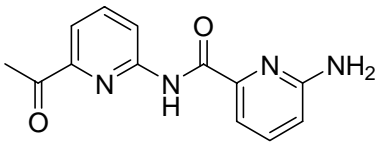
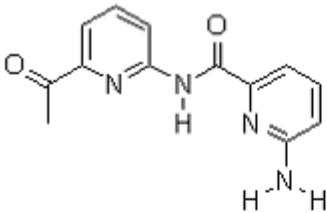
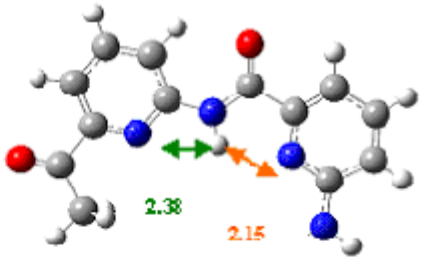
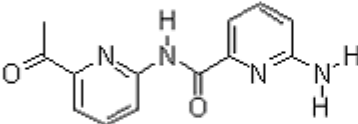
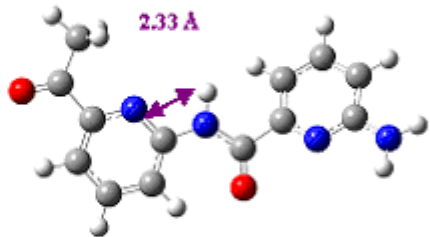
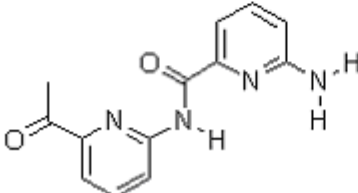
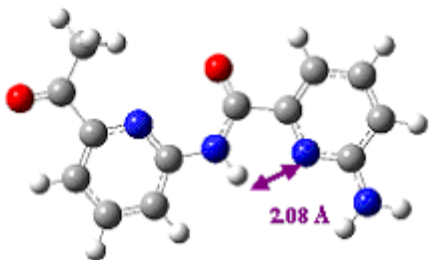
 2			
Conformer	Structure of Conformer	<i>Ab initio</i> calculated structure	Relative energy / Kcal mol ⁻¹
2a			0.0
2b			12.3
2c			8.3

Figure 2.2. *Ab initio* results of three different conformers of dimer 2.

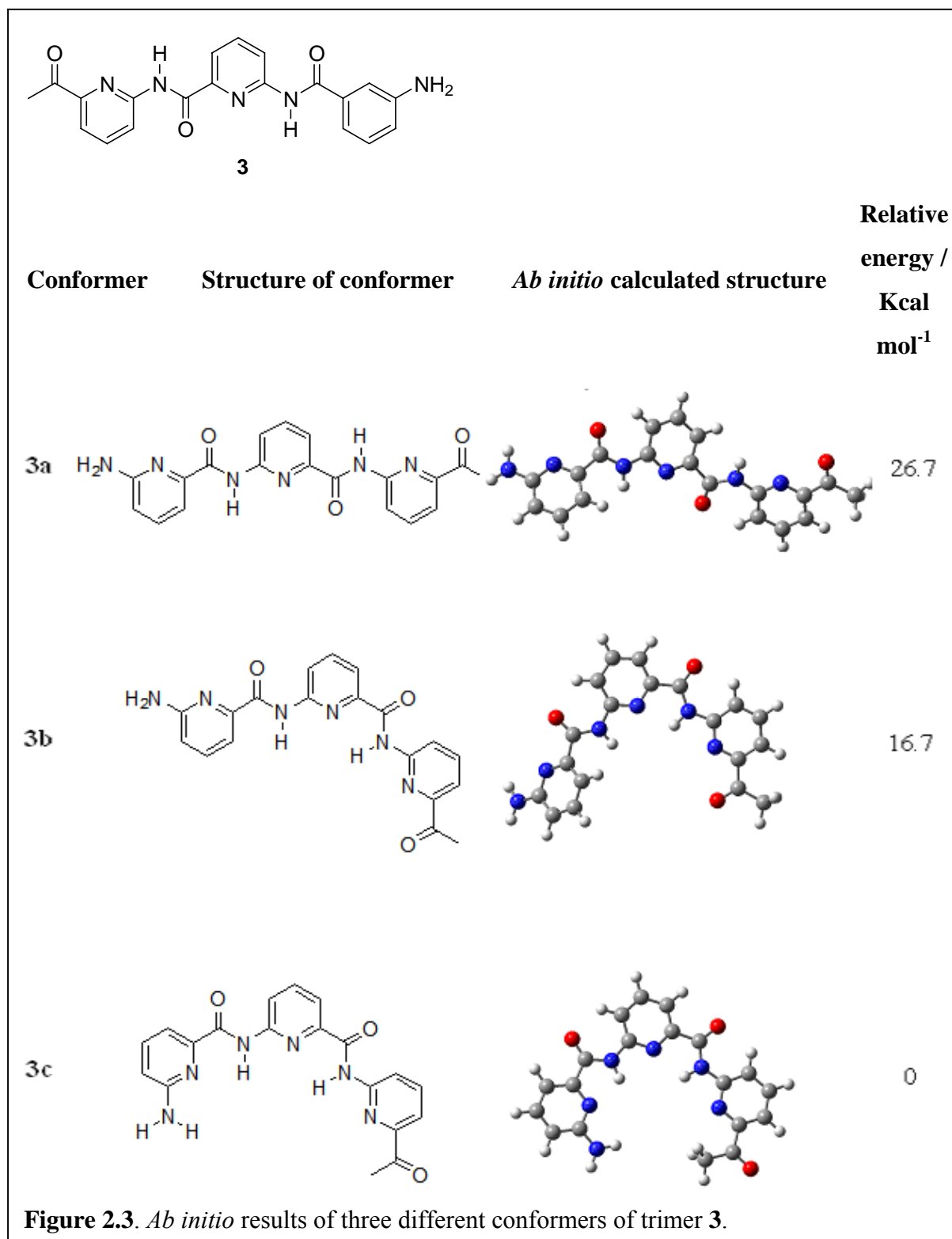
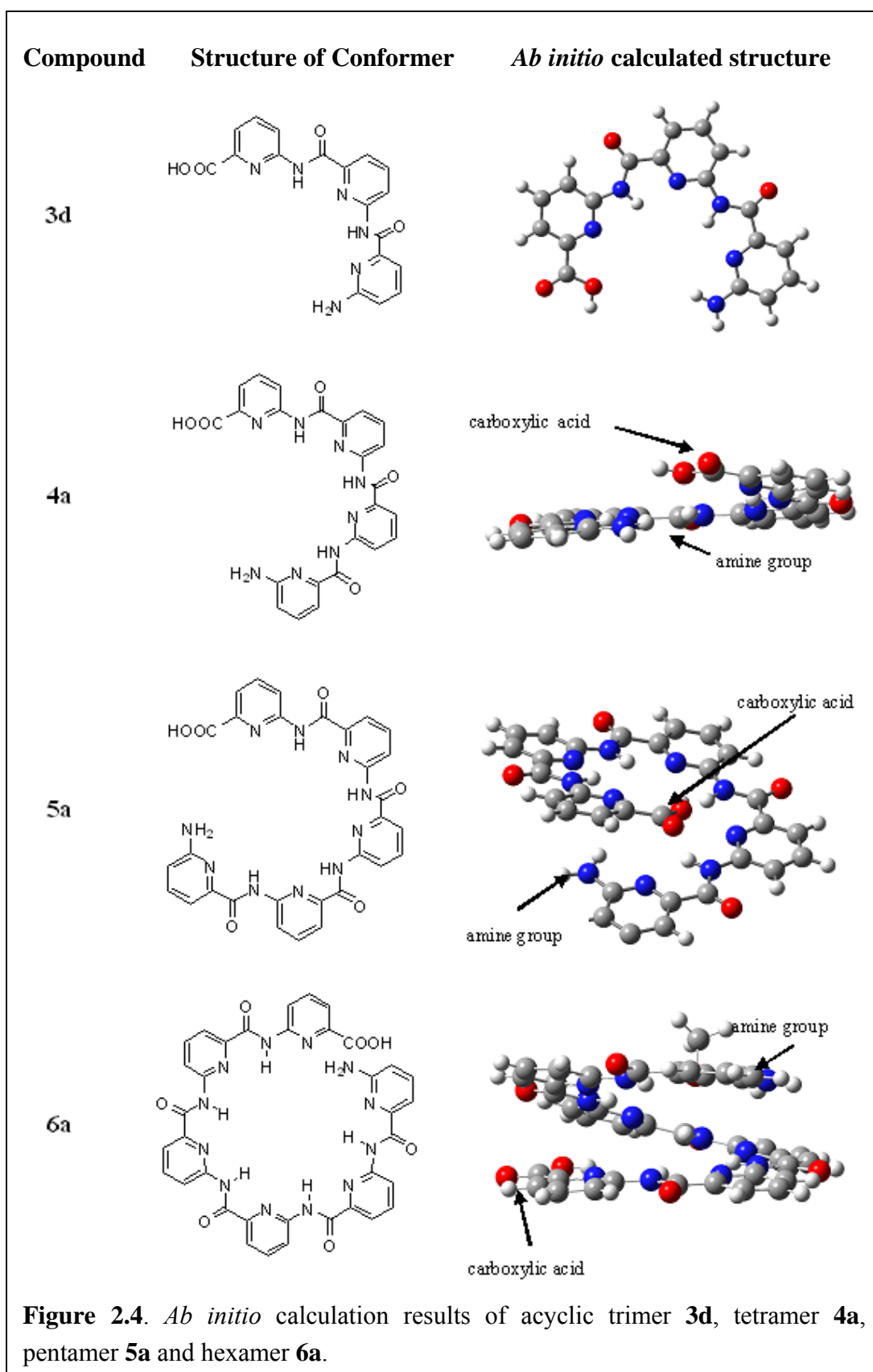
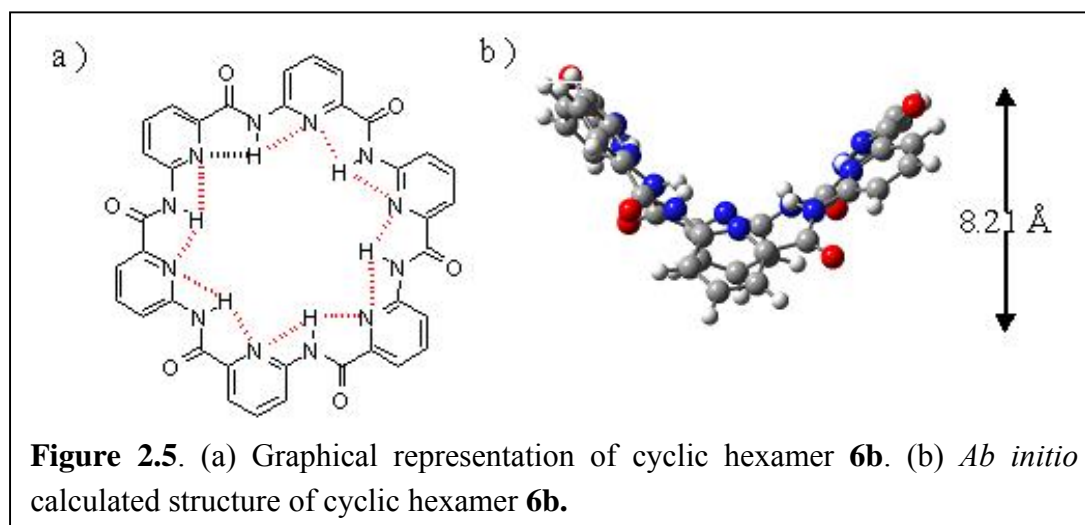


Figure 2.3. *Ab initio* results of three different conformers of trimer **3**.

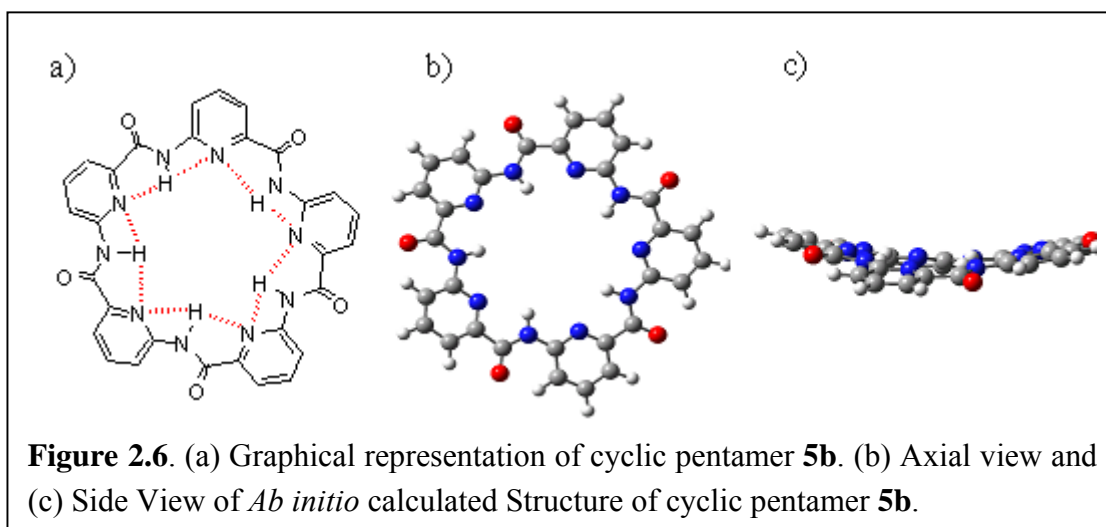


2.2.4 Cyclic Hexamer 6b



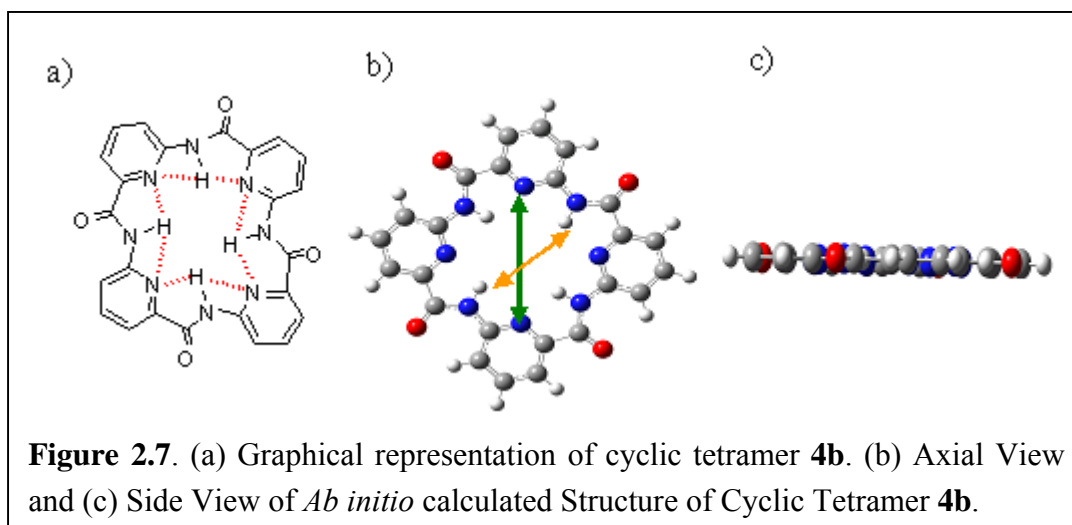
As shown in **Figure 2.5**, the cyclic hexamer **6b** is very strained having a thickness of 8.21 Å. The strained backbone suggests the likelihood of synthetic difficulties. As shown in **Figure 2.4**, the linear hexamer **6a** adopts a helical structure in which the carboxylic acid group and the amine group lie at the opposite end of the helix, indicating that successful coupling of the two functional groups might be synthetically challenging. Additionally, a bent conformation is highly undesirable in our approach toward the development of functional ion channels and thus the cyclic hexamer **6b** is not chosen as the synthetic target.

2.2.5 Cyclic Pentamer 5b



Ab initio calculation of the cyclic pentamer **5b** (Figure 2.6) showed the interior cavity dimension of 7.69 Å at the widest and 5.99 Å at the narrowest. This suggests that ion may be able to transverse the cavity of the cyclic pentamer **5b**. The thickness of pentamer **5b** was estimated to be about 4.8 Å. Similar to the cyclic hexamer **6b**, the strained backbone found in the pentamer **5b** indicates the likelihood of synthetic difficulties. Although the carboxylic acid and amine functional groups at the two terminal pyridine groups are near (Figure 2.4), the distance between them is still relatively large and coupling reaction between the two end groups may be difficult. Despite of this, the synthesis of pentamer was still pursued and cyclization was attempted with repetitive failures.

2.2.6 Cyclic tetramer **4b**



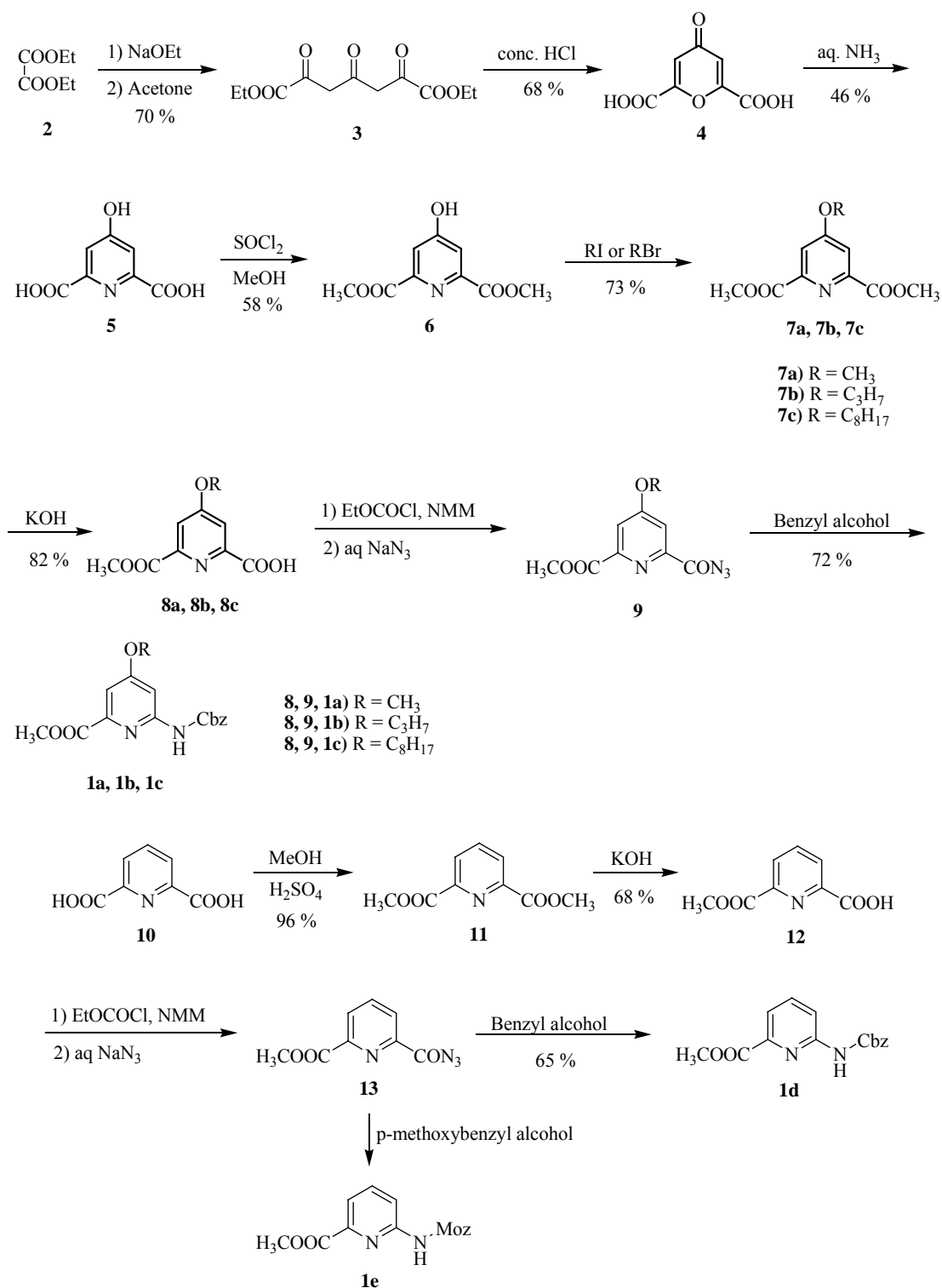
As shown in **Figure 2.7**, the cavity of the optimized cyclic tetramer **4b** is 6.21 Å (green arrow) at the widest and 4.53 Å (orange arrow) at the narrowest. Cyclic tetramer **4b** adopts a planar structure, indicating the absence of molecular strain that may be seen in the cyclic pentamer **5b** and hexamer **6b**. *Ab initio* calculation of the optimized acyclic tetramer **4a** (**Figure 2.4**) shows that the carboxylic acid group on one end and the amine group on the other end are in close proximity that should facilitate the cyclization reaction. Accordingly, the cyclic tetramer **4b** was chosen as the synthetic target and a synthetic route was devised that may enable the synthesis of the cyclic tetramer **4b** (**Figure 2.7**).

2.3 Experimental Section

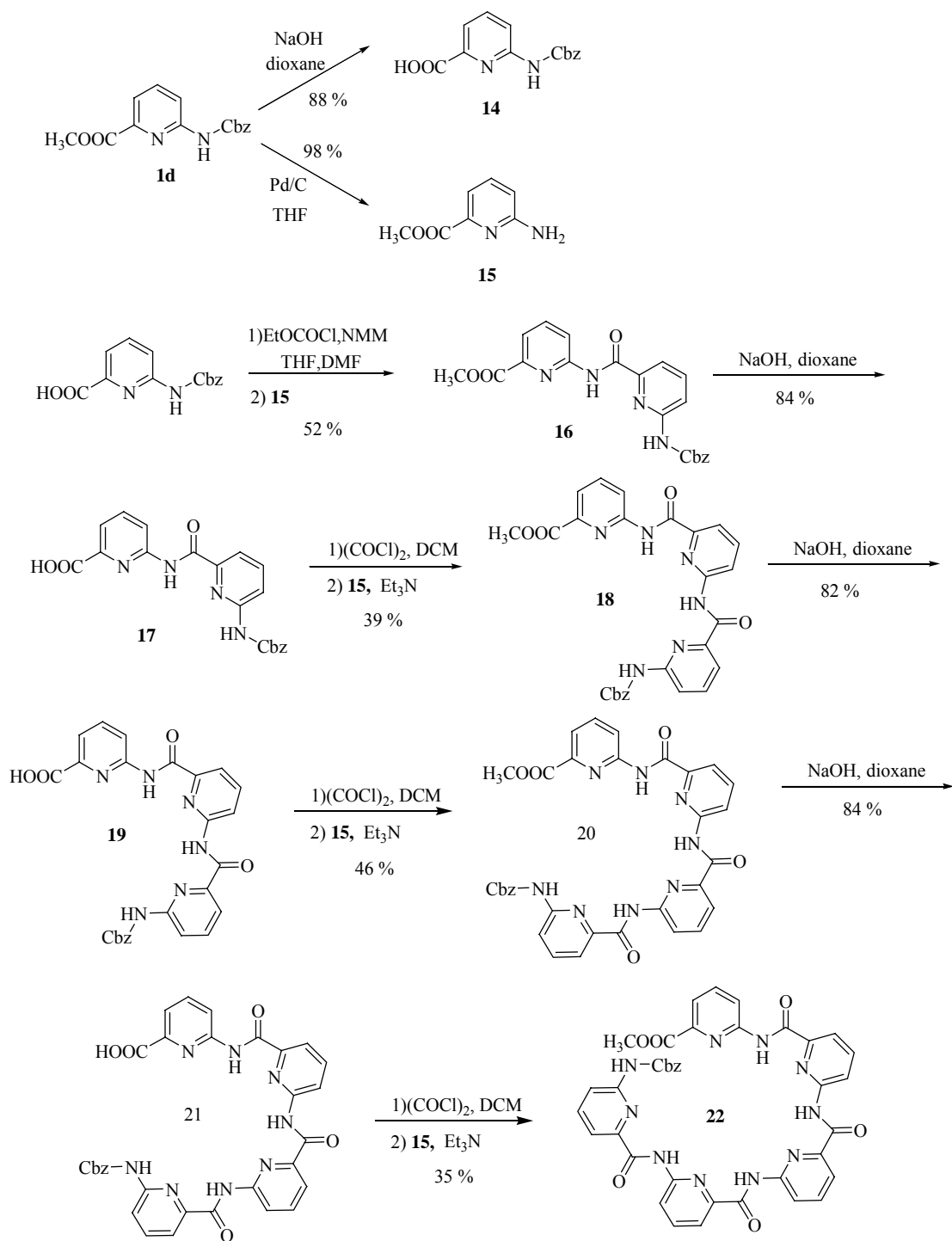
2.3.1 General Remarks

All the reagents were obtained from commercial suppliers and used as received unless otherwise noted. Aqueous solutions were prepared from distilled water. The organic solutions from all liquid extractions were dried over anhydrous Na_2SO_4 for a minimum of 15 minutes before filtration. Reactions were monitored by thin-layer chromatography (TLC) on silica gel precoated glass plates (0.25 mm thickness, 60F-254, E. Merck). Flash column chromatography was performed using pre-coated 0.2 mm silica plates from Selecto Scientific. Chemical yields refer to pure isolated substances. ^1H and ^{13}C NMR spectra were recorded on either a Bruker ACF-300 or ACF-500 spectrometer. In addition, key compounds were characterized by 2D NOSEY and X-ray Diffraction. ^1H NMR spectra were recorded on Bruker ACF300 (300 MHz) and ACF500 spectrometers (500 MHz). The solvent signal of CDCl_3 was referenced at $\delta = 7.26$ ppm. Coupling constants (J values) are reported in Hertz (Hz). ^1H NMR data are recorded in the order: chemical shift value, multiplicity (s, singlet; d, doublet; t, triplet; q, quartet; m, multiplet; br, broad), number of protons that gave rise to the signal and coupling constant, where applicable. ^{13}C spectra are proton-decoupled and recorded on Bruker ACF300 (300 MHz) and ACF500 spectrometers (500 MHz). The solvent, CDCl_3 , was referenced at $\delta = 77$ ppm. CDCl_3 (99.8%-Deuterated) was purchased from Aldrich and used without further purification.

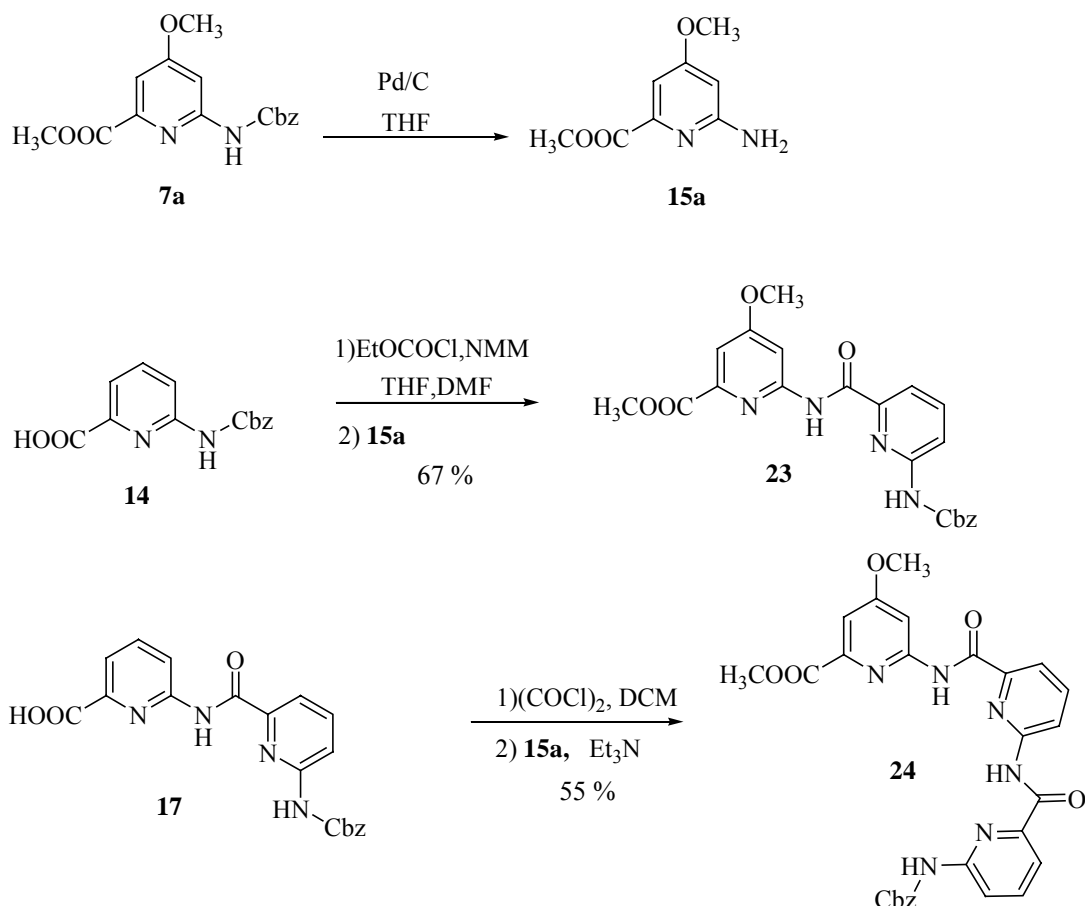
2.3.2 Synthetic Scheme



Scheme 1. Synthesis of monomers 1 & 7.



Scheme 2. Synthesis of trimer **18**, tetramer **20** and pentamer **22** for 2D NOESY study.



Scheme 3. Synthesis of dimer **23** and trimer **24** for structural study in solid state.

2.3.3 Synthetic Procedure

2,4,6-trioxo-1,7-diethylheptanedioate (3): Sodium (1.53 g, 66.50 mmol) was stirred in 30 ml of anhydrous ethanol for 1 hr. The reaction mixture was then heated (60°C–70°C) until all the sodium dissolved. The prepared sodium ethoxide was divided into two portions. Diethyl oxalate (5.30 g, 36.30 mmol) was added to the first portion of sodium ethoxide, stirred and kept warm for later use. The second portion was stirred until precipitation occurs, with which a mixture of acetone (1.93 g, 33.30 mmol) and diethyl oxalate (5.00 g, 34.20 mmol) was added to it immediately and stirred till

precipitation occurs again. Thereafter, the first portion was added to it and stirred for 0.5 hr. The mixture was then allowed to stand overnight. After the removal of the solvent under reduced pressure, 25.00 g of ice and 10 ml of concentrated hydrochloric acid was added to it, stirred, filtered, washed with cold water and dried to give the pure product as a yellow solid (5.90 g, 70%). ^1H NMR (500 MHz, CDCl_3): δ 6.37 (s, 4H), 4.37 (q, 4H, $J = 7.1$ Hz), 1.38 (t, 6H, $J = 7.2$ Hz); ^{13}C NMR (500 MHz, CDCl_3): δ 196.36, 162.03, 161.51, 103.97, 62.74, 14.03; MS-ESI: calculated for $[\text{M}]^+$ ($\text{C}_{11}\text{H}_{14}\text{O}_7$): 257.1, found: 257.1.

Chelidonic acid (4): 10 ml of concentrated hydrochloric acid was added to 5.90 g (22.90 mmol) of **3** and the mixture was heated for 20 hrs at 100°C , filtered, washed with cold water and dried to give the pure product as a light brown solid (4.00 g, 68%). ^1H NMR (500 MHz, DMSO-d_6): δ 6.95 (s, 2H); ^{13}C NMR (500 MHz, DMSO-d_6): δ 179.27, 160.77, 153.92, 118.91; MS-ESI: calculated for $[\text{M}]^+$ ($\text{C}_7\text{H}_4\text{O}_6$): 182.9, found: 182.9.

4-hydroxypyridine-2,6-dicarboxylic acid (5): 20 ml of 10% ammonia solution was added to 4.00 g (21.70 mmol) of **4** and the mixture was heated for 5 hrs at 100°C . Activated charcoal was then added to decolorize the solution. The mixture was filtered and a portion of the ammonia and water in the residue was removed under

reduced pressure, the pH was then adjusted to about 2 – 3 using hydrochloric acid. The reaction mixture was allowed to stand, which was then filtered, and a white solid was recrystallized from water to give the pure product (1.30 g, 46%). ¹H NMR (500 MHz, DMSO-d₆): δ 7.46 (s, 2H); ¹³C NMR (500 MHz, DMSO-d₆): δ 168.64, 164.75, 148.42, 114.77; MS-ESI: calculated for [M]⁺(C₁₄H₁₀N₂O₁₀): 365.0, found: 365.0.

Dimethyl-4-hydroxypyridine-2, 6- dicarboxylate (6): 144 ml of thionyl chloride was added slowly to a stirred mixture of 71.80 g (0.36 mol) of **5** and 720 ml of methanol in an ice-salt bath for 1 hr. After which the ice-salt bath was removed and the mixture was stirred at room temperature for 2 days. The solvent was removed under reduced pressure yielding the pure product as a white solid. (35.90 g, 58 %). ¹H NMR (500 MHz, DMSO-d₆): δ 7.62 (s, 2H), 3.87 (s, 6H); ¹³C NMR (500 MHz, DMSO-d₆): δ 166.09, 164.82, 149.21, 115.31, 52.56; MS-ESI: calculated for [M]⁺(C₉H₉NO₅) m/z: 211.8, found: m/z 211.8.

Dimethyl-4-methoxypyridine-2,6-dicarboxylate (7a): A mixture of 1.69 g (8 mmol) of **6**, 2.00 g (14.50 mmol) of K₂CO₃ and 0.5 ml (8.00 mmol) of iodomethane in 40 ml of anhydrous acetone was refluxed for 24 hrs. The solid was filtered off and the solvent was removed under reduced pressure. The residue was dissolved in CH₂Cl₂ (100 ml) and washed with water twice. The solvent was removed under reduced

pressure and a white solid was recrystallized from methanol to give the pure product.

(1.32 g, 73 %). ^1H NMR (500 MHz, CDCl_3): δ 7.80 (s, 2H), 4.00 (s, 6H), 3.97 (s, 3H);

^{13}C NMR (500 MHz, CDCl_3): δ 167.62, 165.15, 149.82, 114.12, 56.03, 53.21; MS-

ESI: calculated for $[\text{M}]^+$ ($\text{C}_{10}\text{H}_{11}\text{NO}_5$): m/z 226.0, found: 226.0.

4-methoxy-6-(methoxycarbonyl)picolinic acid (8a): 1.51 g (27.00 mmol) of potassium hydroxide, which was dissolved in 6 ml of water, was added dropwise into a flask containing 6.08 g (27.00 mmol) of **7a** in 300 ml of methanol. After stirring the mixture for 6 hrs at room temperature, most of the solvent was removed under reduced pressure. The remaining solution was then poured into a separating funnel containing water and CH_2Cl_2 . The aqueous layer was washed with CH_2Cl_2 to remove the unreacted starting material. 100 ml of 1 M HCl was then added to the aqueous layer and the crude product was extracted using CH_2Cl_2 . Recrystallization from methanol yields the pure product as a white solid. (4.68 g, 82%). ^1H NMR (500 MHz, DMSO-d_6): δ 13.47 (br, 1H), 7.71 (d, 1H, $J = 2.5$ Hz), 7.70 (d, 1H, $J = 2.6$ Hz), 3.96 (s, 3H), 3.90 (s, 3H); ^{13}C NMR (500 MHz, DMSO-d_6): δ 167.02, 165.53, 164.71, 113.47, 56.16, 52.60; MS-ESI: calculated for $[\text{M}]^+$ ($\text{C}_9\text{H}_9\text{NO}_5$): m/z 212.0, found: 212.0.

6-(methoxycarbonyl)-4-methoxypyridine-2-carboxylic acid (1a): Compound **8a**

(0.21 g, 1.00 mmol) was dissolved in THF (3 ml) and DMF (2 ml). This solution was cooled to -5°C to -10°C using an ice-salt bath. 4-methylmorpholin (0.1 ml, 1.00 mmol) and Ethyl chloroformate (0.1ml, 1.00 mmol) was injected to the cooled solution. It was allowed to stir for 15 minutes. 0.07 g NaN₃ dissolved in minimal amount of water was injected into the cooled solution. It was allowed to stir for 30 minutes. The product was washed with water and extracted with CH₂Cl₂. Solvent was removed in vacuo. A solution of product (0.26 g, 0.90 mmol) and benzyl alcohol (1.17 g, 1.10 mmol) in dry toluene (10 ml) was first heated at 80°C for 2 hours and then further refluxed at 120°C for 30 hours. Solvent was removed in vacuo. The crude product was washed with water and extracted with CH₂Cl₂. Removal of solvent yields a crude compound which was then re-crystallised with MeOH to give a pure product as a white solid. (0.23 g, 72%). ¹H NMR (500MHz, CDCl₃): δ 10.66 (s, 1H), 7.96 (s, 1H), 7.75 (d, 1H, *J* = 2.5 Hz), 7.32–7.36 (m, 5H), 5.19 (s, 2H), 3.91 (s, 3H), 3.89 (s, 3H). ¹³C NMR (500 MHz, CDCl₃): δ 168.29, 165.12, 153.06, 152.99, 147.05, 135.68, 147.05, 135.68, 128.53, 128.27, 127.84, 108.83, 100.10, 67.04, 55.71, 52.80. MS-ESI: calculated for [M]⁺ (C₁₆H₁₆N₂O₅): m/z 316.1 found: m/z 316.0.

Dimethyl pyridine-2, 6-dicarboxylate (11): MeOH (120 ml) was added to compound **1** (5.49 g, 32.90 mmol), followed by dropwise addition of concentrated

H₂SO₄ (5 ml). The solution was heated under refluxing for 48 hours. Solvent was removed in vacuo. The product was washed with water and aqueous NaOH, extracted with CH₂Cl₂. Removal of solvent yields the pure product as a white solid. (6.16g, 96%) ¹H NMR (500MHz, CDCl₃): δ 8.28 (q, 2H, *J* = 3.8 Hz), 7.98–8.02 (m, 1H), 3.99 (s, 6H). ¹³C NMR (500 MHz, CDCl₃): δ 164.9771, 148.1724, 138.2907, 127.9426, 53.0940 MS-ESI: calculated for [M]⁺(C₉H₉NO₄): m/z 195.1 found: m/z 195.2.

6-(methoxycarbonyl)picolinic acid (12): MeOH (300 ml) and solid KOH (1.72 g, 30.70 mmol) dissolved in minimal amount of water were added to compound **11** (6.00 g, 30.70 mmol). The mixture was stirred at room temperature for 12 hours. Solvent was removed in vacuo. The residue was dissolved in water. It was extracted with CH₂Cl₂ twice and solvent was removed in vacuo to yield compound **11**. 1 M HCl was added to the aqueous layer until the pH decrease to pH 1 and below. This acidified aqueous layer was then extracted 10 times with CH₂Cl₂ and removal of solvent give a white product (3.79 g, 68%). ¹H NMR (500 MHz, DMSO-d₆): δ 8.22–8.25 (m, 2H), 8.17 (t, 1 H, *J* = 7.9 Hz), 3.91 (s, 3H). ¹³C NMR (500 MHz, DMSO-d₆): δ 165.62, 147.57, 139.06, 127.86, 55.61. MS-ESI: calculated for [M]⁺(C₈H₇NO₄): m/z 181.0 found: m/z 181.2.

Methyl 6-(benzyloxycarbonyl)picolinate (1d): Compound **12** (0.18 g, 1.00 mmol) was dissolved in THF (3 ml) and DMF (2 ml). This solution was cooled to -5°C to -10°C using an ice-salt bath. Ethyl chloroformate (0.1ml, 1.00 mmol) and 4-methylmorpholin (0.1 ml, 1.00 mmol) was injected to the cooled solution. It was allowed to stir for 15 minutes. 0.07 g NaN₃ dissolved in minimal amount of water was injected into the cooled solution. It was allowed to stir for 30 minutes. The product was washed with water and extracted with CH₂Cl₂. Solvent was removed in vacuo. The crude azide was crystallized using hexane. It was then filtered and the residue was dried in vacuo to give a pure beige product. A solution of acid chloride (0.26 g, 0.90 mmol) and benzyl alcohol (1.17 g, 1.10 mmol) in dry toluene (10 ml) was first heated at 80°C for 2 hours and then further refluxed at 120°C for 30 hours. Solvent was removed in vacuo. The crude product was washed with water and extracted with CH₂Cl₂. Removal of solvent yields a crude compound which was then re-crystalised with MeOH to give a pure product **1d** as a white solid (0.17g, 65%). ¹H NMR (500MHz, CDCl₃): δ 8.19 (q, 1H, *J* = 6.9 Hz), 8.06 (s, 1H), 7.79 (m, 2H), 7.30–7.35 (m, 5H), 5.19 (s, 2H), 3.91 (s, 3H). ¹³C NMR (500 MHz, CDCl₃): δ 165.06, 152.96, 151.47, 145.86, 139.19, 135.62, 128.49, 128.24, 127.89, 120.25, 116.12, 67.07, 50.95. MS-ESI: calculated for [M]⁺(C₁₅H₁₄N₂O₄): m/z 286.1 found: m/z 286.1.

6-(benzyloxycarbonyl)picolinic acid (14): Dioxane (10 ml) was added to compound **1d** (0.57 g, 2.00 mmol) into round bottom flask. Solid NaOH (0.16 g, 4.00 mmol) was

dissolved in minimal amount of de-ionized water, which was then added into the content of the round bottom flask. It was allowed to stir at room temperature for 1 day. Solvent was removed in vacuo. Water (20 ml) and MeOH (20 ml) was added, followed by KHSO₄ (0.54 g, 4.00 mmol). The suspension was then filtered and the residue was obtained and then dried under IR lamp to give a pure product **14** as a white solid (0.48 g, 88%). ¹H NMR (500MHz, DMSO-d₆): δ 10.56 (s, 1H), 8.04 (d, 1H, *J* = 8.9 Hz), 7.94 (t, 1H, *J* = 7.9 Hz), 7.69–7.71 (m, 1H), 7.37–7.43 (m, 4H), 7.31–7.34 (m, 1H), 5.19 (s, 2H). ¹³C NMR (500 MHz, DMSO-d₆): δ 165.95, 153.70, 152.09, 147.20, 139.30, 132.36, 128.42, 127.92, 127.64, 115.85, 112.44, 65.82. MS-ESI: calculated for [M]⁺(C₁₄H₁₂N₂O₄): m/z 272.1 found: m/z 272.2.

Methyl 6-aminopicolinate (15): Compound **1** (0.29 g, 1.00 mmol) was reduced by catalytic hydrogenation in THF (10 ml) at 50°C for 3 hours, using Pd/C (0.03 g, 10% of the weigh of compound **1**) as the catalyst. The reaction mixture was then filtered and the solvent was removed in vacuo to give the crude product **15**. This was directly used in the next step without further purification. (0.15g, 98%) ¹H NMR (500MHz, DMSO-d₆): δ 7.51 (t, 1H, *J* = 7.9 Hz), 7.18 (d, 1H, *J* = 7.6 Hz), 6.50 (d, 1H, *J* = 8.2 Hz), 6.29 (s, 2H), 3.79 (s, 3H). ¹³C NMR (500 MHz, DMSO-d₆): δ 165.79, 159.70, 145.70, 137.69, 113.20, 112.24, 51.88.

Methyl 6-(2-(benzyloxycarbonyl)picolinamido)picolinate (16): THF (3 ml) and DMF (2 ml) were added to compound **14** (0.27 g, 1.00 mmol) in a round bottom flask placed in an ice bath. 4-methylmorpholin (0.1 ml, 1.00 mmol) and ethyl chloroformate (0.1 ml, 1.00 mmol) were added to the round bottom flask and stirred for 30 minutes, while maintaining the temperature at -5°C to -10°C. Compound **15** (0.15g, 1.00 mmol) was dissolved in DCM (2 ml) and DMF (2 ml) and this solution was then injected into the round bottom flask in the ice bath. Then the round bottom flask was removed from the ice bath and was allowed to stir at 90°C under reflux overnight. Solvent was then removed in vacuo and the product was washed with water and extracted with CH₂Cl₂. Removal of solvent yield a crude compound which was then re-crystalised with MeOH with refluxed for 1 hour to give a pure product **16** as a white solid (0.21g, 52%). ¹H NMR (500 MHz, DMSO-d₆): 10.96 (s, 1H), 10.46 (s, 1H), 8.54 (d, 1H, *J* = 8.2 Hz), 8.05–8.14 (m, 3H), 7.87 (d, 2H, *J* = 7.0 Hz), 7.35–7.46 (m, 5H), 5.23 (s, 2H), 3.90 (s, 3H). ¹³C NMR (500 MHz, DMSO-d₆): 164.64, 162.13, 153.45, 151.31, 150.75, 146.07, 140.43, 140.10, 136.35, 128.45, 128.05, 127.86, 121.14, 117.09, 116.85, 116.01, 66.08, 52.49, 48.58. MS-ESI: calculated for [M]⁺(C₂₁H₁₈N₄O₅): m/z 406.1 found: m/z 406.2.

6-(2-(benzyloxycarbonyl)picolinamido)picolinic acid (17): Dioxane (10 ml) was added to compound **16** (0.81 g, 2.00 mmol) into round bottom flask. Solid NaOH

(0.16 g, 4.00 mmol) was dissolved in minimal amount of de-ionized water, which was then added into the content of the round bottom flask. It was allowed to stir at room temperature for 1 day. Solvent was removed in vacuo. Water (20 ml) and methanol (20 ml) was added, followed by KHSO₄ (0.54 g, 4.00 mmol). The suspension was then filtered and the residue was obtained and then dried under IR lamp to give a pure product **17** as a white solid. (0.69g, 84%) ¹H NMR (500 MHz, DMSO-d₆): δ 10.94 (s, 1H), 10.45 (s, 1H), 8.50 (s, 1H), 7.88–8.48 (m, 3H), 7.82–7.86 (m, 2H), 7.33–7.45 (m, 5H), 5.24 (s, 1H), 3.81 (s, 1H). ¹³C NMR (500 MHz, DMSO-d₆): δ 162.67, 162.33, 153.49, 151.26, 150.48, 147.54, 146.88, 140.88, 140.57, 139.92, 136.37, 128.64, 128.26, 128.07, 121.07, 121.08, 118.78, 117.12, 116.14, 66.38. MS-ESI: calculated for [M]⁺(C₂₀H₁₆N₄O₅): m/z 392.1 found: m/z 392.1.

Methyl 6-(2-(2-(benzyloxycarbonyl)picolinamido)picolinamido)picolinate (18):

Acid **17** (0.39 g, 1.00 mmol) was placed in a very dry round bottom flask and saturated with nitrogen gas. Freshly-prepared dry CH₂Cl₂ (10 ml) and DMF (0.1 ml) were added to the acid, followed by dropwise addition of oxalyl chloride (0.3 ml, 2.00 mmol). The reaction mixture was allowed to stir for 2 hours. The solvent was then removed in vacuo and protected under nitrogen before addition of 10mL dry CH₂Cl₂. Minimal amount of CH₂Cl₂ was added to dissolve compound **15** (0.15 g, 1.00 mmol), which was followed by addition of triethylamine (0.1 ml, 0.30 mmol) and DMAP (0.02 g, 10% weight of compound **15**). This was then injected into acid chloride. It

was allowed to stir room temperature for 1 hour. The product was washed with water and extracted with CH₂Cl₂. Solvent was then removed in vacuo and purification was done with flash column chromatography (10 : 1 v/v CH₂Cl₂ : EA) to give a pure product **18** as a white solid (0.21g, 39%) ¹H NMR (500MHz, CDCl₃): δ 10.44 (s, 1H), 10.30 (s, 1H), 8.70–8.74 (m, 2H), 8.31 (d, 1H, *J* = 8.1 Hz), 7.91–8.08 (m, 7H), 7.35–7.44 (m, 5H), 5.26 (s, 2H), 3.90 (s, 3H); ¹³C NMR (500 MHz, CDCl₃): δ 165.28, 162.58, 162.43, 151.37, 150.59, 150.02, 147.05, 140.05, 139.50, 128.61, 128.46, 128.40, 121.44, 118.833, 118.08, 117.92, 117.54, 116.04, 67.51, 52.95, 30.90. MS-ESI: calculated for [M]⁺(C₂₇H₂₂N₆O₆): m/z 526.2 found: m/z 526.1.

6-(2-(2-(benzyloxycarbonyl)picolinamido)picolinamido)picolinic acid (19):

Dioxane (10 ml) was added to compound **18** (1.05 g, 2.00 mmol) into round bottom flask. Solid NaOH (0.16 g, 4.00 mmol) was dissolved in minimal amount of de-ionized water, which was then added into the content of the round bottom flask. It was allowed to stir at room temperature for 1 day. Solvent was removed in vacuo. Water (20 ml) and MeOH (20 ml) was added, followed by KHSO₄ (0.54 g, 4.00 mmol). The suspension was then filtered and the residue was obtained and then dried under IR lamp to give a pure product **19** as a white solid. (0.84g, 82%) ¹H NMR (500MHz, DMSO-d₆): δ 10.70 (s, 1H), 10.58 (s, 1H), 10.23 (s, 1H), 8.42–8.50 (m, 2H), 7.78–8.11 (m, 7H), 7.32–7.43 (m, 5H), 5.23(s, 2H). ¹³C NMR (500 MHz, DMSO-d₆): δ

165.87, 162.41, 162.06, 153.03, 151.13, 150.44, 149.91, 147.33, 146.68, 140.53, 140.27, 139.74, 136.26, 128.49, 128.10, 127.96, 127.77, 123.17, 121.02, 118.58, 117.29, 116.87, 116.80, 115.88, 66.23. MS-ESI: calculated for $[M]^+(C_{26}H_{20}N_6O_6)$: m/z 512.1 found: m/z 512.1.

Methyl 6-(2-(2-(2-(benzyloxycarbonyl)picolinamido)picolinamido)picolinamido)-picolinate (20): Compound **19** (0.51 g, 1.00 mmol) was allowed to be in the nitrogen atmosphere. 10 ml CH_2Cl_2 and 0.1 ml of DMF were subsequently added, followed by addition of oxalyl chloride (0.3 ml, 2.00 mmol). The solution was stirred for 4 hours at room temperature. Solvent was removed in vacuo and the resulting acid chloride was dissolved in dry CH_2Cl_2 (10 ml). Minimal amount of CH_2Cl_2 was added to dissolve compound **15** (0.15 g, 1.00 mmol), which was followed by addition of triethylamine (0.1 ml, 0.30 mmol) and 4-dimethylaminopyridine (0.02 g, 10% weight of compound **15**). This was then injected into acid chloride. It was allowed to stir at room temperature for 1 hour. The product was washed with water and extracted with methylene chloride. Solvent was then removed in vacuo and purification was done with flash column chromatography (10 : 1 v/v CH_2Cl_2 : EA) to give a pure product **10** as a white solid (0.29 g, 46%). 1H NMR (500MHz, $CDCl_3$): δ 10.56 (s, 1H), 10.40(s, 1H), 10.32 (s, 1H), 8.55–8.63 (m, 4H), 8.22 (d, 1H, $J = 8.2$ Hz), 7.88–8.03 (m, 6H), 7.72–7.79 (m, 2H), 7.05–7.19 (m, 5H), 4.99 (s, 2H), 3.80 (s, 3H). ^{13}C NMR (500

MHz, CDCl₃): δ 164.87, 162.43, 162.33, 153.07, 151.23, 150.69, 149.95, 149.83, 147.20, 147.14, 147.00, 145.70, 140.04, 139.97, 139.46, 135.25, 128.35, 128.35, 128.12, 127.54, 121.07, 118.71, 118.66, 117.73, 117.65, 117.39, 116.06, 67.00, 52.78. MS-ESI: calculated for [M]⁺(C₃₃H₂₆N₈O₇): m/z 646.2 found: m/z 646.2.

6-(2-(2-(2-(benzyloxycarbonyl)picolinamido)picolinamido)picolinamido)picolinic

acid (21): Dioxane (10 ml) was added to compound **20** (1.29 g, 2.00 mmol) into round bottom flask. Solid NaOH (0.16 g, 4.00 mmol) was dissolved in minimal amount of de-ionized water, which was then added into the content of the round bottom flask. It was allowed to stir at room temperature for 1 day. Solvents were removed in vacuo. Water (20 ml) and MeOH (20 ml) was added, followed by KHSO₄ (0.54 g, 4.00 mmol). The suspension was then filtered and the residue was obtained and then dried under IR lamp to give a pure product **21** as a white solid (1.07 g, 84%).

¹H NMR (500MHz, DMSO-d₆): δ 11.06 (s, 1H), 10.68 (s, 1H), 10.61 (s, 1H), 10.57 (s, 1H), 8.55–8.48 (m, 3H), 8.19–7.84 (m, 9H), 7.25–7.19 (m, 5H), 5.06 (s, 2H). ¹³C NMR (500 MHz, DMSO-d₆): δ 165.66, 163.29, 162.33, 162.28, 153.23, 151.18, 150.65, 150.19, 149.92, 148.36, 147.26, 146.61, 140.57, 140.52, 140.43, 139.74, 135.98, 128.21, 127.78, 120.99, 118.49, 117.67, 116.85, 115.97, 66.13. MS-ESI: calculated for [M]⁺(C₃₂H₂₄N₈O₇): m/z 632.2 found: m/z 632.2.

Methyl 6-(2-(2-(2-(2-(benzyloxycarbonyl)picolinamido)picolinamido)-

picolinamido)picolinamido)picolinate (22): Compound **21** (0.63 g, 1.00 mmol) was allowed to be in the nitrogen atmosphere. 10 ml CH₂Cl₂ and 0.1 ml of DMF were subsequently added, followed by addition of oxalyl chloride (0.3 ml, 2.00 mmol). The solution was stirred for 4 hours at room temperature. Solvent was removed in vacuo and the resulting acid chloride was dissolved in dry CH₂Cl₂ (10 ml). Minimal amount of CH₂Cl₂ was added to dissolve compound **15** (0.15 g, 1.00 mmol), which was followed by addition of triethylamine (0.1 ml, 0.30 mmol) and 4-dimethylaminopyridine (0.02 g, 10% weight of compound **15**). This was then injected into acid chloride. It was allowed to stir at room temperature for 1 hour. The product was washed with water and extracted with methylene chloride. Solvent was then removed in vacuo and purification was done with flash column chromatography (10 : 1 v/v CH₂Cl₂ : EA) to give a pure product **22** as a white solid (0.27g, 35 %). ¹H NMR (500 MHz, DMSO-d₆): δ 10.61 (s, 1H), 10.55 (s, 1H), 10.50 (s, 1H), 10.42 (s, 1H), 8.70–8.75 (m, 1H), 8.61–8.63 (m, 1H), 8.22 (s, 1H), 7.94–8.10 (m, 5H), 7.67–7.83 (m, 7H), 7.11–7.16 (m, 3H), 7.02 (d, 2H, *J* = 7.0 Hz), 6.88 (s, 1H), 5.00 (s, 2H), 3.58 (s, 3H). ¹³C NMR (500 MHz, DMSO-d₆): δ 168.10, 164.20, 162.67, 162.47, 162.45, 162.30, 152.82, 152.28, 150.18, 149.96, 147.27, 146.74, 140.25, 140.15, 139.50, 135.22, 128.32, 128.01, 118.76, 118.45, 117.53, 117.36, 117.32, 117.12, 149.97,

110.39, 101.01, 67.31, 55.91. MS-ESI: calculated for $[M]^+(C_{39}H_{30}N_{10}O_8)$: m/z 766.2
found: m/z 766.5.

Methyl 6-(2-(benzyloxycarbonyl)-4-methoxypicolinamido)picolinate (23): THF (3 ml) and DMF (2 ml) were added to compound **14** (0.30 g, 1.00 mmol) in a round bottom flask placed in an ice bath. 4-methylmorpholin (0.1 ml, 1.00 mmol) and ethyl chloroformate (0.1 ml, 1.00 mmol) were added to the round bottom flask and stirred for 30 minutes, while maintaining the temperature at -5°C to -10°C . Compound **15a** (0.15 g, 1.00 mmol) was dissolved in CH_2Cl_2 (2 ml) and DMF (2 ml) and this solution was then injected into the round bottom flask in the ice bath. Then the round bottom flask was removed from the ice bath and was allowed to stir at 90°C under reflux overnight. Solvent was then removed in vacuo and the product was washed with water and extracted with CH_2Cl_2 . Removal of solvent yield a crude compound which was then recrystallised with MeOH with reflux for 1 hour to give a pure product **23** as a white solid. (0.29 g, 67%) ^1H NMR (500 MHz, CDCl_3): δ 10.34 (s, 1H), 8.24 (d, 1H, $J = 5.6$ Hz), 8.20 (d, 1H, $J = 7.6$ Hz), 7.89–7.94 (m, 2H), 7.62 (s, 1H), 7.35–7.47 (m, 7H), 5.28 (s, 1H), 4.00 (s, 3H), 3.96 (s, 3H). ^{13}C NMR (500 MHz, DMSO-d_6): δ 168.37, 165.29, 162.38, 152.86, 152.74, 150.23, 1147.27, 147.04, 140.04, 135.68, 128.64, 128.39, 127.97, 117.65, 115.82, 109.79, 101.66, 101.60, 67.33, 55.86, 52.98. MS-ESI: calculated for $[M]^+(C_{22}H_{20}N_4O_6)$: m/z 437.4 found: m/z 437.3.

Methyl 6-(2-(2-(benzyloxycarbonyl)-4-methoxypicolinamido) picolinamido)-picolinate (24): Compound **17** (0.42 g, 1.00 mmol) was allowed to be in the nitrogen atmosphere. 10 ml CH₂Cl₂ and 0.1 ml of DMF were subsequently added, followed by addition of oxalyl chloride (0.3 ml, 2.00 mmol). The solution was stirred for 4 hours at room temperature. Solvent was removed in vacuo and the resulting acid chloride was dissolved in dry CH₂Cl₂ (10 ml). Minimal amount of CH₂Cl₂ was added to dissolve compound **15a** (0.15 g, 1.00 mmol), which was followed by addition of triethylamine (0.1 ml, 3.00 mmol) and DMAP (0.02 g, 10% weight of compound **15**). This was then injected into acid chloride. It was allowed to stir at room temperature for 1 hour. The product was washed with water and extracted with CH₂Cl₂. Solvent was then removed in vacuo and purification was done with flash column chromatography (10 : 1 v/v CH₂Cl₂ : EA) to give a pure product **25** as a white solid (0.31 g, 55%) ¹H NMR (500MHz, CDCl₃): δ 10.39 (br, 1H), 10.28 (br, 1H), 8.70 (d, 1H, *J* = 13.5 Hz), 8.68 (d, 2H, *J* = 1.9 Hz), 7.94–8.05 (m, 5H), 7.50 (d, 1H, *J* = 3.8 Hz), 7.36–7.42 (m, 5H), 5.26 (s, 2H), 3.99 (s, 3H), 3.88 (s, 3H). ¹³C NMR (500 MHz, CDCl₃): δ 168.43, 165.33, 162.69, 162.45, 152.99, 152.92, 150.58, 147.31, 147.17, 147.05, 140.10, 140.07, 135.51, 128.62, 128.49, 128.45, 118.78, 117.57, 116.05, 110.04, 102.04, 92.90, 92.78, 67.55, 55.93, 53.06. MS-ESI: calculated for [M]⁺(C₂₈H₂₄N₆O₇): m/z 557.5 found: m/z 557.3.

2.4 Results and Discussion

2.4.1 Synthesis of the monomer and higher oligomers

The preparation of monomers was shown in **Scheme 1** and each of them with different side chains, and monomer **1d** was prepared from diethyl oxalate and pyridine-2, 6-dicarboxylic acid, respectively, through a series of reactions which include cyclization, esterification, alkylation, hydrolysis and Curtius rearrangement. There are a few important points to be highlighted for the synthetic route. Firstly, two different methods were employed for the esterification of **5** to **6** and **10** to **11**. Although the method where concentrated sulfuric acid was used the catalyst yielded a high chemical yield, the same method can not be applied to the esterification of **5**. Secondly, in the hydrolysis reaction, the amount of acid used for the neutralization should be approximately equivalent to that of sodium hydroxide used in the reaction to prevent the protonation of the nitrogen atom on the pyridine ring. Lastly, the synthesis of higher oligomers was generally achieved by coupling the acid group of the oligomers to the amine group of the monomer **15** (not between acid of the monomer with the amine of the oligomer). This is due to the poor solubility of the amine-containing oligomers higher than dimer in common organic solvents.

2.4.2 X-ray Crystal Structure Analysis

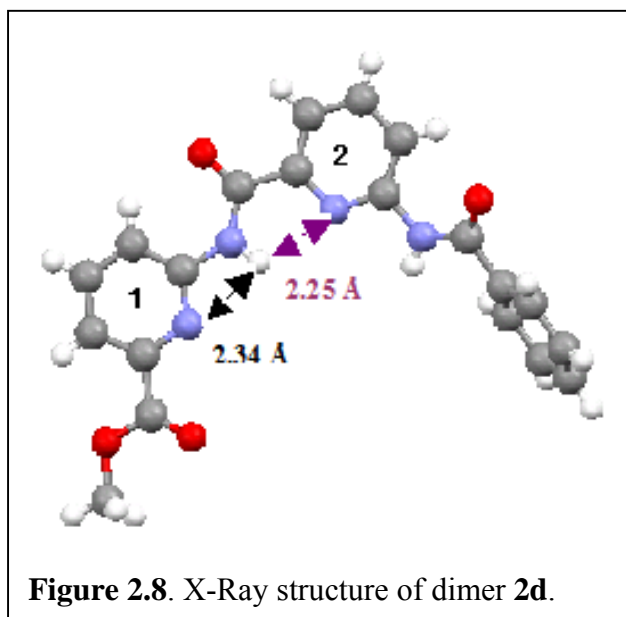
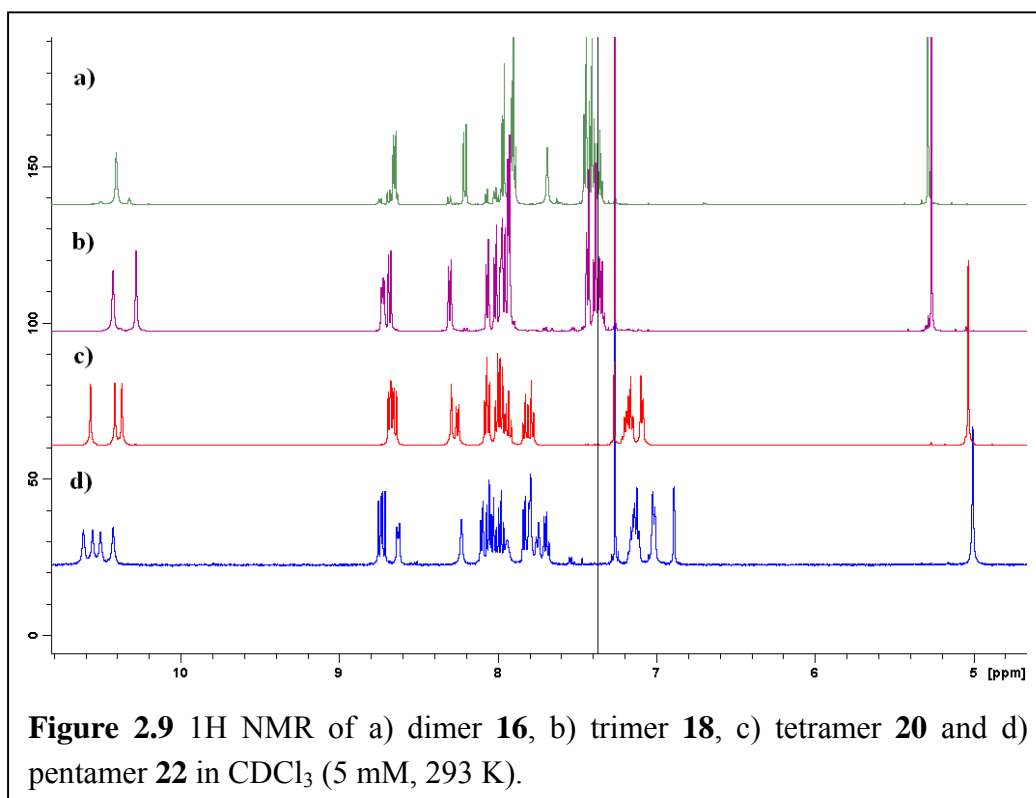


Figure 2.8 showed the X-Ray structure of the dimer **2d** (synthesized and crystallized by Changliang Ren). It showed the expected crescent conformation curved toward the hydrogen-bonded side in solid state. The overall molecule, excluding the

terminal benzene group, is flat and planar with a rigid, crescent backbone. The twisting around the terminal benzene ring may be due to the crystal packing. The distance in the four-membered hydrogen bond is 2.34 Å, which is close to that of 2.38 Å predicted by *ab initio* calculation. Similarly, the distance in the five-membered hydrogen bond is 2.25 Å, which is close to that of 2.16 Å predicted by *ab initio* calculation. The X-Ray results show that intramolecular hydrogen bonds are indeed present in dimer, which gives rise to a rigidified backbone with an expected crescent configuration.

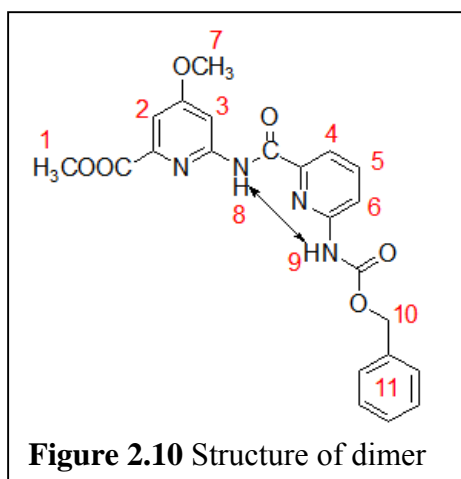
2.4.3 1D ^1H NMR for Oligomers

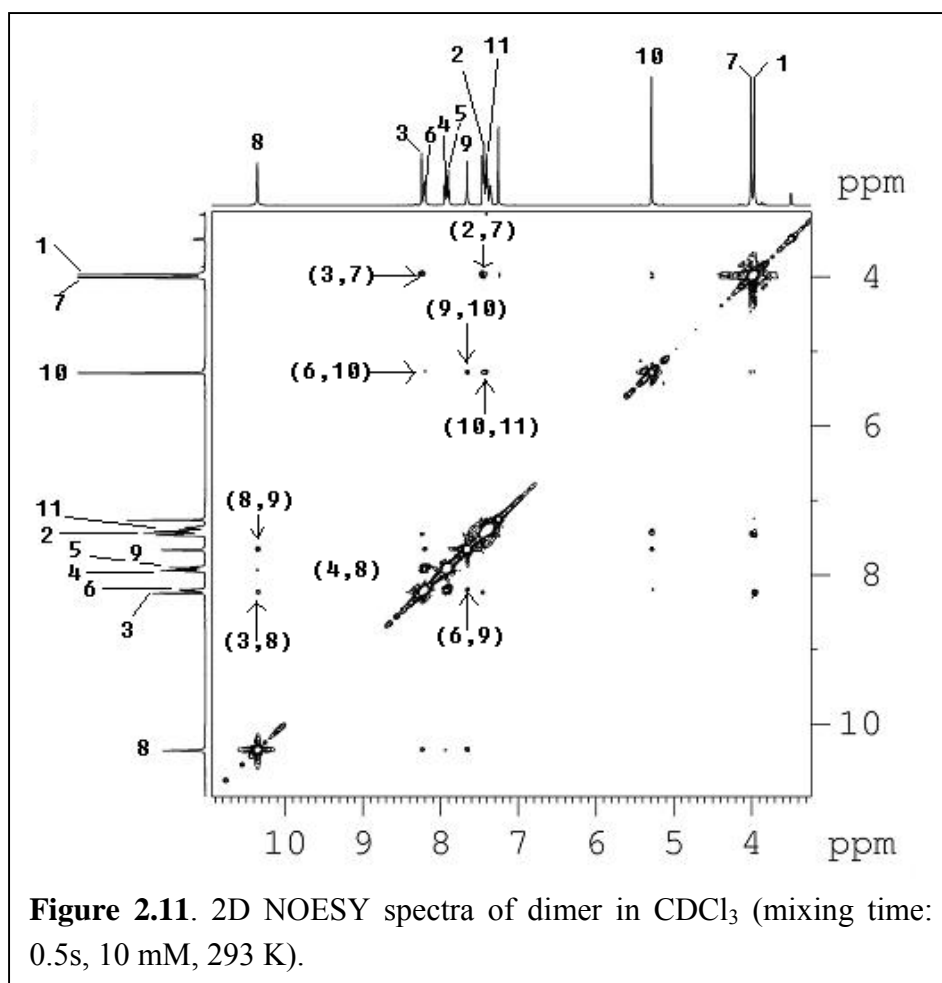


2.4.4 2D NOESY Results

With the positive results obtained from X-ray analysis, 2D NOESY experiments were performed on the oligomers to see whether the curved conformation persists in solution or not.

Dimer



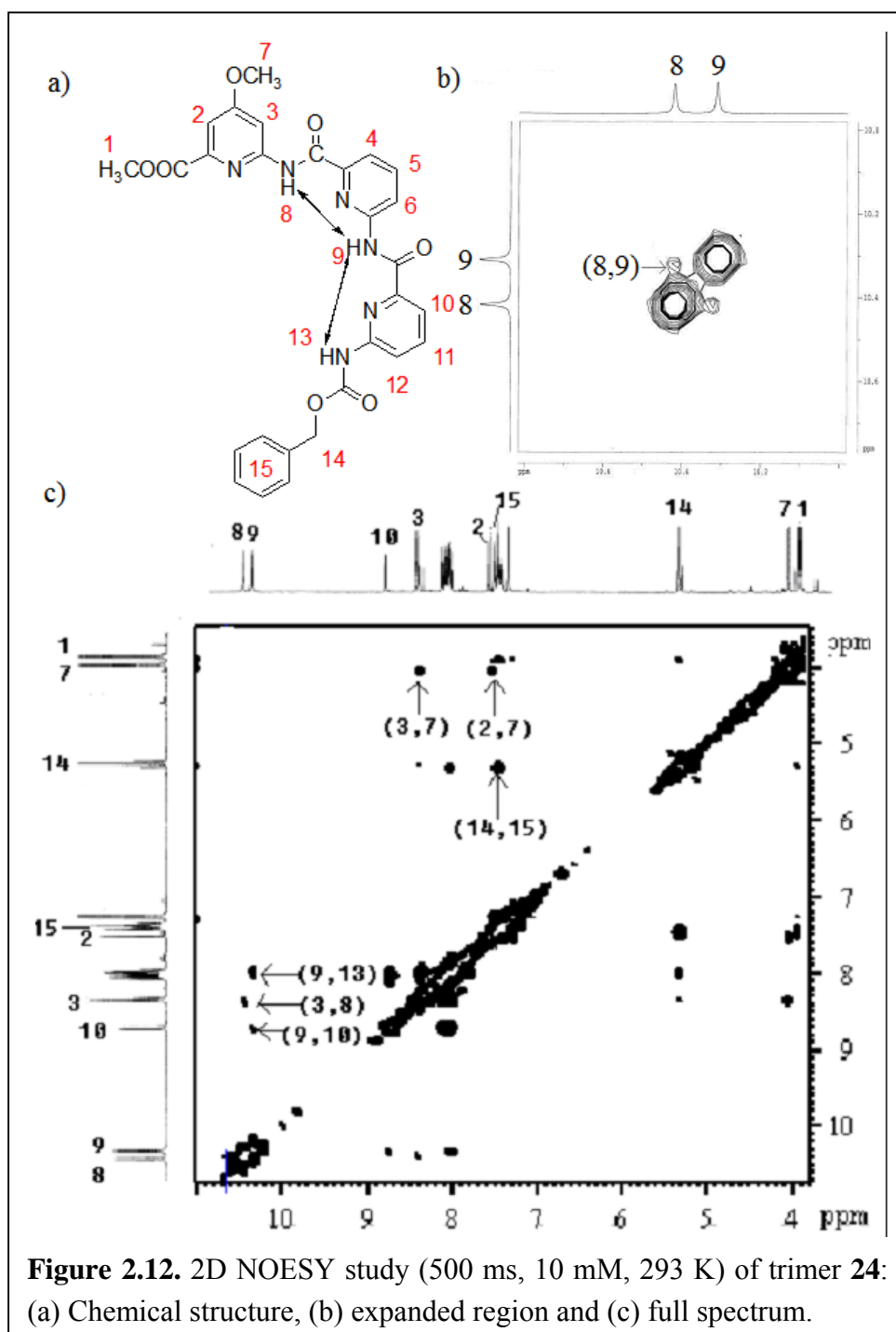


In the 2D NOESY spectrum of dimer **23** in CDCl_3 at 300 K (**Figure 2.11**), a strong NOE contact between amide protons 8 and 9 was observed, indicating that a crescent configuration was adopted in solution.

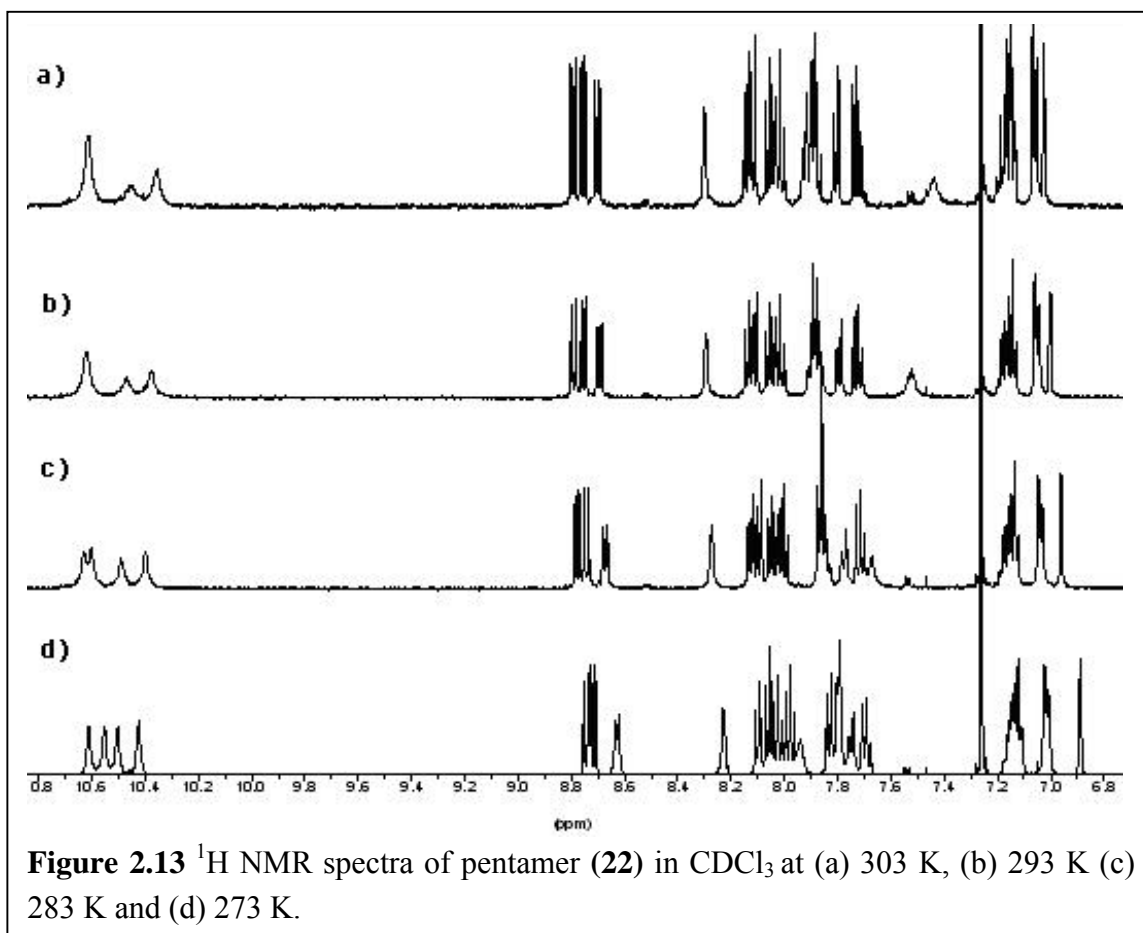
Trimer

Similarly, in the 2D NOESY spectrum of the trimer **24** in CDCl_3 at 293K (**Figure 2.12**), two NOE cross peaks were observed among the three amide protons present in the molecules, consistent with a crescent configuration adopted by trimer

24 in solution. These two observations are in agreement with the *ab initio* calculations performed earlier.



2.4.5 Variable Temperature ^1H NMR Study on Pentamer **22**



As shown in **Figure 2.11b**, the ^1H NMR spectrum of pentamer **22** at room temperature contains overlap of some signals and not well-defined amide protons (10.2 - 10.6 ppm). These hamper the elucidation of the folded structure of **22** in solution by 2D NOESY study. We thought that a change in temperature may lead to a better dispersion in proton NMR signals. A variable temperature ^1H NMR study on pentamer **22** was then carried out. **Figure 2.13d** showed that while the four amide protons in pentamer **22** were separated well at 273 K, there is no much improvement on the aromatic region due to the highly repeating nature of the pentamer. Despite this,

2D NOESY was still carried out that didn't give out any NOE crosspeaks that are indicative of the folded conformation adopted by **22** in solution.

2.4.6 Binding Study by Dilution Method

The chemical shifts of the amide protons in different concentrations in solution were monitored using NMR. The dilution experiments were carried out on a series of diluted solutions of 1:1 complex of the oligomers and the anions through nonlinear regression analysis. The ^1H NMR dilution experiments of Cbz-protected trimer and tetramer in the presence of the anion salts such as TBACl, TBABr and TBAI were performed to examine the anion binding by pyridine oligomers.

The solutions were prepared by the well-established dilution method in the supramolecular chemistry and the procedures for the experiments were as follows:

- (a) Oligomer/salts (1:1 ratio, 1.4 ml) were prepared in CDCl_3 to make a 20 mM solution.
- (b) 0.7 ml of the 20 mM solution was added into 0.7 ml of CDCl_3 and mixed well using a vortex mixer to give a 10 mM solution (1.4 ml).
- (c) The procedure (b) was repeated to make solutions of 5 mM, 2.5 mM, 1.25 mM, 0.625 mM and 0.3125 mM, respectively.

(d) The ^1H NMR spectrum was recorded for all the above solutions and the chemical shifts of amide protons were plotted against concentrations and fitted according to equation (1) to determine the association constants between host and guest.

The association constant (K_s) of the oligomers with the anions were calculated from the equation (1) below using the chemical shift of the amide protons observed in the ^1H NMR.

$$\delta = \delta_0 + \Delta\delta_{\max} \left\{ 1 + (2K_s C)^{-1} - [(2K_s C)^{-2} + (K_s C)^{-1}]^{1/2} \right\} \quad (1)$$

where δ = experimentally observed chemical shift of oligomer;

δ_0 = chemical shift of unbound oligomer which is treated as a constant;

$\Delta\delta = \delta_{\text{complex}} - \delta_{\text{oligomer}} =$ difference in chemical shift of oligomer in fully complexed and unbound forms;

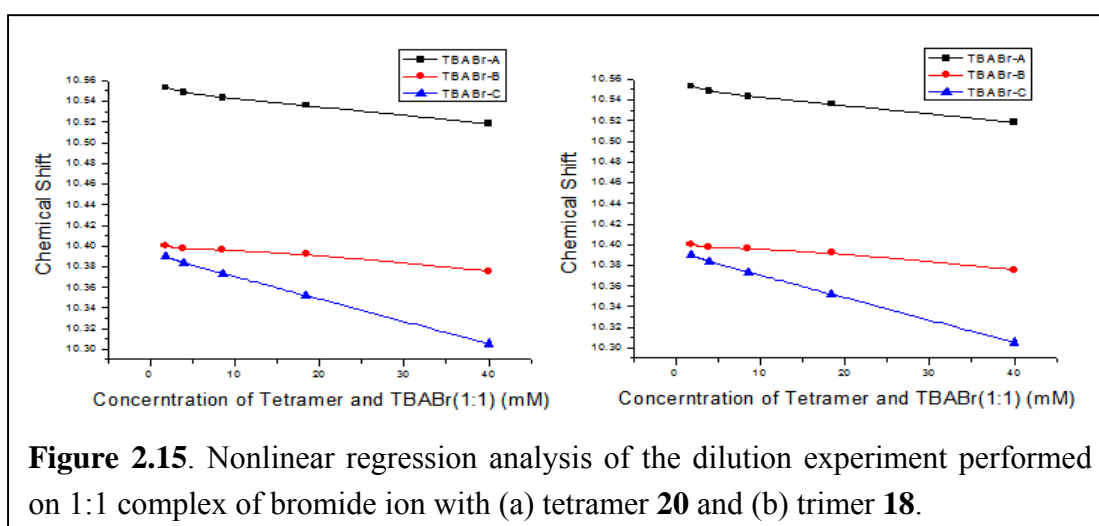
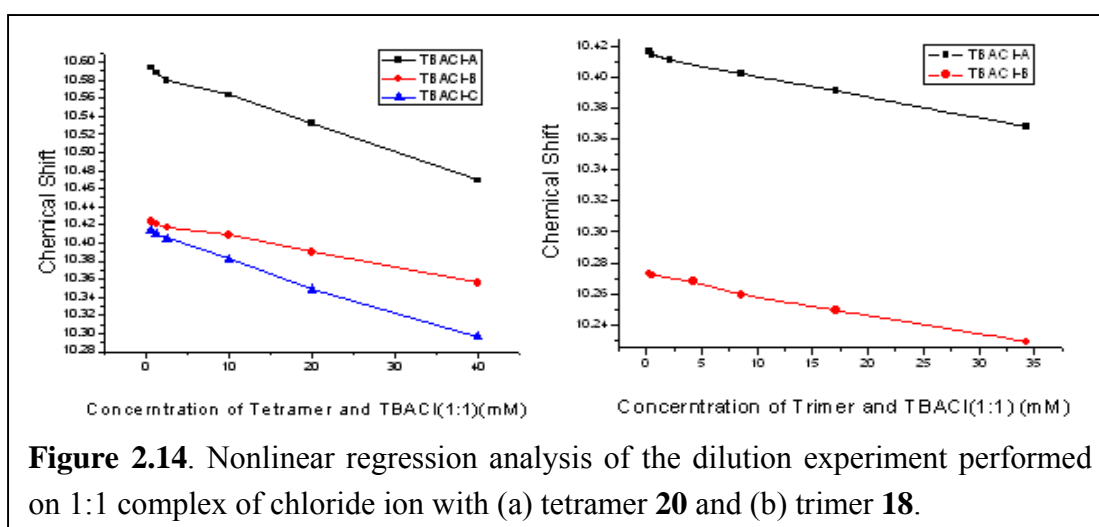
K_s = association constant;

C = A series of diluted total concentration.

δ & C can be experimentally determined from the NMR whereas δ_0 , $\Delta\delta_{\max}$ and K_s or K_d are constants that will be derived from nonlinear regression analysis.

Figures 2.14-2.16 and **Table 2.1** showed the plotted curves of the chemical shifts of the amide protons of the oligomers versus the concentrations and the determined association constants with the anions. We observed that the K_s values obtained from every amide protons are smaller than 0.01 in all cases that suggest to us

that the pyridine oligomers do not bind to chloride, bromide and iodide anions. Similar results were obtained when other anions such as tetrabutylammonium acetate, tetrabutylammonium thiocyanate, tetrabutylammonium trifluoromethanesulfonate, tetrabutylammonium hydrogen sulfide, tetrabutylammonium nitrate were tested. No binding between the anions and the oligomers could be observed possibly due to (1) the smaller cavity size that can not accommodate even the smallest anions (e.g., Cl⁻) and (2) the strong hydrogen bonding interactions among amide protons and pyridine nitrogen atoms that prevent the amide protons from sticking out to hydrogen bond to anions.



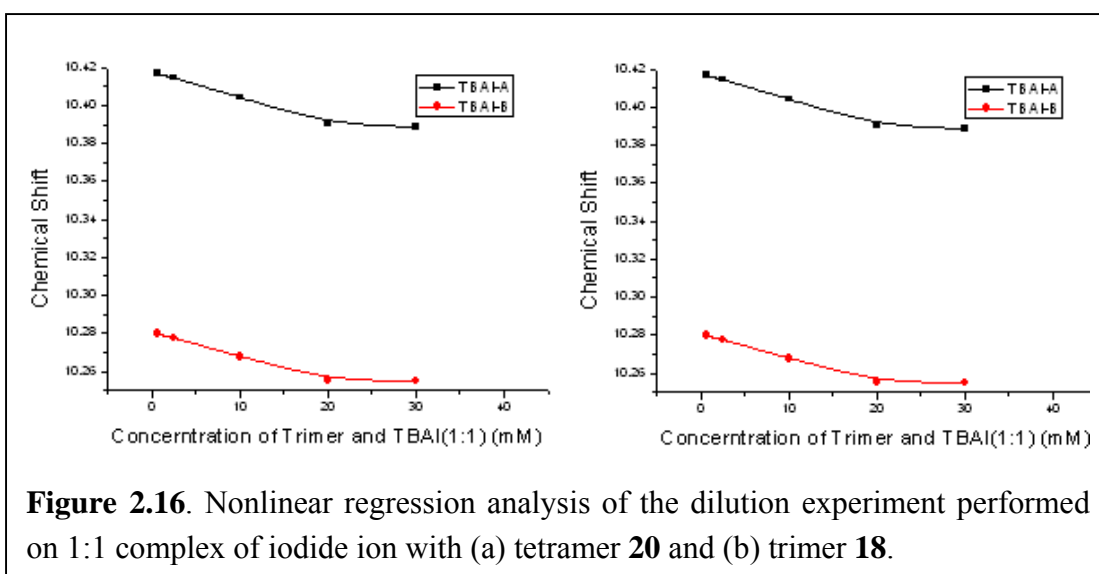


Table 2.1. Association constants of tetramer and trimer with iodide.

Anion	Amide proton	δ_0	$\Delta\delta_{\max}$	Ks
Tetramer	A	10.58984 ± 0.00088	-1.59971 ± 0.57725	0.00184 ± 0.00076
		10.42026 ± 0.00061	-1.41471 ± 0.87917	0.0012 ± 0.00082
	C	10.41153 ± 0.00068	-1.08916 ± 0.18978	0.00296 ± 0.00063
Trimer	A	10.41898 ± 0.00309	-0.09887 ± 0.0562	0.02352 ± 0.02662
	B	10.28206 ± 0.00311	-0.07808 ± 0.03955	0.03102 ± 0.03519

2.5 Conclusion

Pyridine-based crescent aromatic γ -peptides were designed where a continuous intramolecular hydrogen-bonding network was introduced into the molecule so as to rigidify the amide backbone through hydrogen bonding forces. The restricted rotational freedom of the aryl-amide bonds then gives rise to a crescent configuration with its interior cavity decorated by amide protons and pyridine nitrogen atoms.

A synthetic route was developed that permits the synthesis of pyridine-based aromatic foldamers. 2D NOESY studies and X-Ray crystallography analysis confirmed the crescent conformation be adopted by these oligomers not only in solution but also in solid state, which was remarkably reproducible by the *ab initio* calculations.

The synthesized acyclic trimer and tetramer were tested for their binding affinities toward various anions, e.g., chloride, bromide, iodide, hydrogen sulfide, nitrate, acetate, thiocyanate and trifluoromethanesulfate and no appreciable binding can be observed for oligomers of up to tetramer.

References:

1. Davis, A. P.; Sheppard, D. N.; Smith, B. D. *Chem. Soc. Rev.* **2002**, 36, 343.
2. Wallace, D. P.; Tomich, J. M., Iwamoto, T.; Henderson K.; Grantham, J. J.; Sullivan L. P. *Am. J. Physiol.: Cell Physiol.* **1997**, 272, C1672.
3. Wallace, D. P.; Tomich, J. M., Eppler, J. W.; Iwamoto, T.; Grantham, J. J.; Sullivan L. P. *Biochim. Biophys. Acta.* **2000**, 69, 1464.
4. Reddy, G. L.; Iwamoto, T.; Tomich, J. M.; Montal, M. *J. Biol. Chem.* **1993**, 268, 14608.
5. Hill, D. J.; Mio, M. J.; Prince, R. B.; Hughes, T. S.; Moore, J. S.; *Chem Rev.* **2001**, 101, 3893.
6. Gellman, S. H. *Acc. Chem. Res.* **1998**, 31, 173.
7. Gong, B.; Zhu, J.; Parra, R. D.; Zeng, H. ; Ewa, S. J. ; Zeng X. C. *J. Am. Chem. Soc.* **2000**, 122, 4219.
8. Gong, B.; Yuan, L.; Zeng, H.; Yamato, K.; Sanford, A. R.; Feng, W.; Atreya, H. S.; Sukumaran, D. K.; Szyperski, T. *J. Am. Chem. Soc.* **2004**, 126, 16528.
9. Gong, B.; Yuan, L.; Sanford, A. R.; Feng, W. Zhang, A.; Zhu, J.; Zeng, H.; Yamato, K.; Li, M.; Ferguson, J. S. *J. Org. Chem.* **2005**, 70, 10660.

Chapter Three

New Method for Demethylation of Aryl Methyl Ether

3.1 Introduction

The protection of phenol moiety as its methyl ether is an important methodology used in organic chemistry. The very high stability of the aryl methyl ether moiety under various conditions makes it very difficult to be deprotected. Consequently, there had been many methods developed over the years for the efficient regeneration of aromatic hydroxyl group from aromatic methoxy group under mild conditions particularly in the presence of other reactive or sensitive functional groups. Studies on steric and electronic factors on the removal of alkyl groups in various aryl alkyl ethers by Chakraborti showed that aryl methyl ether has a higher stability than other alkyl groups and thus is difficult to be removed.¹ In another study performed on the anisole derivatives by Koutek, an increased reaction rate in demethylation correlates well with the presence of electron withdrawing groups present on the anisole ring. However, this protocol was not very practical as high temperature of 180°C and long reaction time were required for the demethylation reaction.²

Many groups had developed different demethylation protocols via nucleophilic, oxidative or reductive mechanisms over the years. Some reagents used include sodium cyanide-dimethyl sulfoxide, which is particularly useful for the

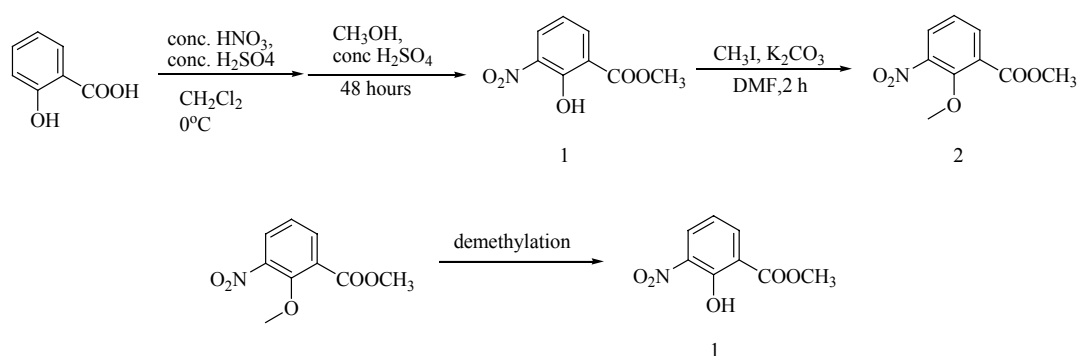
aromatic methoxy nitriles³, toluene radical anion⁴, ethanethiolate anion⁵, benzenethiolate anion⁶, *in situ* generated thiophenolate anion⁷, trifluoroacetic acid and hydrogen bromide. Despite of the significant progress made so far, there are very few methods mild enough for the efficient cleavage of aromatic ether linkage in the presence of some sensitive functional groups.

Our initial interest in demethylation arose from the need of converting aromatic methyl ether into phenol in some methoxybenzene-based aromatic pentamers as represented by **5** (**Scheme 5**) under mild conditions. Under some previously reported demethylation conditions using such as DMSO, NaCN and HBr, the pentamer decomposed, possibly forming linear oligomers of different lengths. Chakraborti reported the use of thiophenol in *N*-methyl-2-pyrrolidone (NMP) with catalytic amount of potassium fluoride as an efficient procedure for the demethylation reaction under neutral and nonhydrolytic conditions¹; however, this method was not effective for our compound. It was reported in that literature that the solvent NMP may play an important role in the regeneration of the active nucleophile (ArS⁻) in nucleophilic activation¹. We decided to use NMP as the solvent and tried different conditions and reagents in a hope to identify good conditions for removing the interior methoxy methyl groups of the methoxybenzene-derived foldmers. During this trial and error-correction process, we discovered that tetrabutylammonium halide salts could cleave the aryl methyl ether to give the desired phenol moiety.

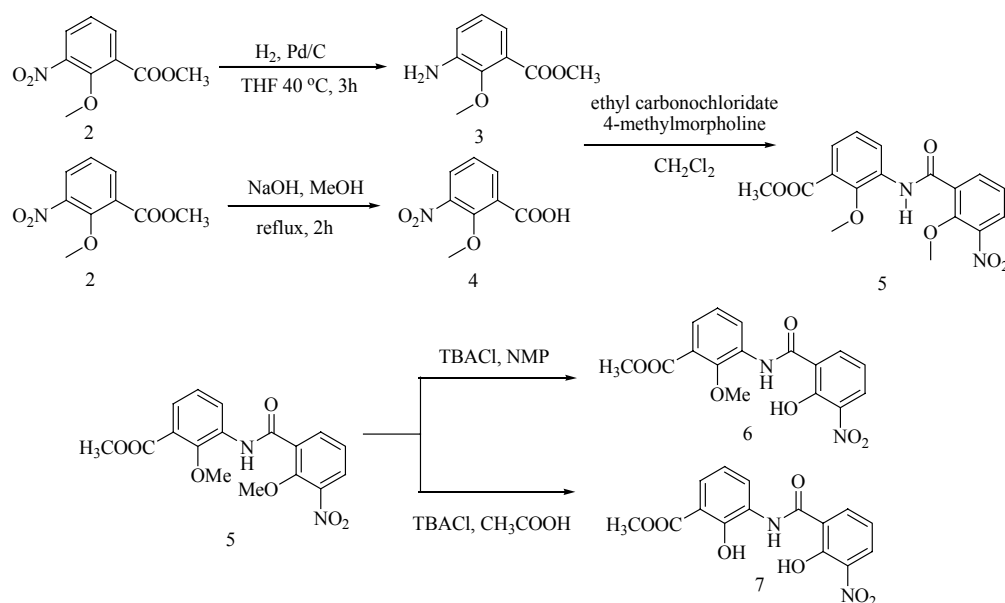
This chapter aims to investigate the scope and limitations of the demethylation reaction promoted by tetrabutylammonium halide salts on some aryl methyl ether compounds under different conditions with the aim of developing a new methodology for the selective demethylation of aromatic ethers.

3.2 Experimental

3.2.1 Synthetic Scheme



Scheme 4. Synthesis of monomer **2** and demethylation.



Scheme 5. Synthesis of dimer **5** and demethylation.

3.2.2 Synthetic Procedure

Methyl 2-hydroxy-3-nitrobenzoate (1): Salicylic acid (10.00 g, 72.50 mmol) was dissolved in 200 ml of CH₂Cl₂, to which concentrated HNO₃ (69 %, 6.1 ml, 94.20 mmol) was added with stirring at 0°C. Concentrated H₂SO₄ (95 %, 10.6 ml, 145.00 mmol) was then added dropwise to the reaction mixture. After 20 min, the reaction was quenched with 500 ml of distilled water and the mixture was filtered. The crude product was dissolved in methanol (250 ml), to which concentrated H₂SO₄ (21.9 ml, 388.00 mmol) was added. The mixture was heated under reflux for 48 hours. The solvent was then removed in *vacuo* and the residue was dissolved in CH₂Cl₂ (200 ml), washed with water (2 x 100 ml), aq. NaHCO₃ (100 ml) and dried over anhydrous Na₂SO₄. Removal of CH₂Cl₂ gave a yellow solid which was purified by gradient flash column chromatography on silica gel (6 : 1 v/v hexane : EA) to give the pure product **1** as a bright yellow solid. Overall Yield: 4.00 g, 28 %. ¹H NMR (300 MHz, CDCl₃): δ 11.99 (s, 1H), 8.13–8.17 (m, 2H), 7.00 (t, 1H, *J* = 4.9 Hz), 4.02 (s, 3H). ¹³C NMR (75 MHz, CDCl₃): δ 169.16, 155.59, 137.97, 135.67, 131.30, 118.34, 115.78, 53.10. MS-ESI: calculated for [M]⁺ (C₈H₇NO₅): *m/z* 197.1, found: *m/z* 197.0.

Methyl 2-methoxy-3-nitrobenzoate (2): Compound **1** (6.00 g, 30.40 mmol) was dissolved in DMF (125 ml) to which anhydrous K₂CO₃ (15.60 g, 112.90 mmol) and iodomethane (6.9 ml, 112.00 mmol) were added. The mixture was heated under reflux

for 4 hours. The reaction mixture was then filtered and the solvent was removed in *vacuo*. The residue was dissolved in CH₂Cl₂ (100 ml), washed with water (2 x 50 ml), and dried over anhydrous Na₂SO₄. Removal of CH₂Cl₂ gave a pure light yellow solid **2**. Yield: 6.41 g, 82 %. ¹H NMR (300 MHz, CDCl₃): δ 8.03 (d, 1H, *J* = 1.8 Hz), 8.00 (d, 1H, *J* = 1.8 Hz), 7.30 (t, 1H, *J* = 1.8 Hz), 3.99 (s, 3H), 3.95 (s, 3H). ¹³C NMR (75 MHz, CDCl₃): δ 164.4, 152.9, 145.17, 135.3, 128.0, 127.1, 123.5, 63.9, 52.4. MS-ESI: calculated for [M]⁺ (C₉H₉NO₅): *m/z* 211.0, found: *m/z* 211.1.

Methyl 3-amino-2-methoxybenzoate (3): Compound **2** (2.00 g, 9.48 mmol) was reduced by catalytic hydrogenation in THF (50 ml) at 40°C, using Pd/C (0.20g, 10%) as the catalyst for 3 hours. The reaction mixture was then filtered and the solvent removed in *vacuo* to give the pure brown liquid **3**. Yield: 1.72g, qualitative.

2-Methoxy-3-nitrobenzoic acid (4): Compound **1** (4.00 g, 19.00 mmol) was dissolved in hot methanol (10 ml) to which 1M NaOH (40 ml, 40.00 mmol) was added. The mixture was heated under reflux for 2 hours and then quenched with water (100 ml). The aqueous layer was neutralized by addition of 1M HCl (80 ml) until the pH was at least 1. The precipitated crude product was collected by filtration, which was recrystallized from hot methanol to give a pure white solid **4**. Yield: 3.45 g, 92 %. ¹H NMR (300 MHz, CDCl₃): δ 8.29 (dd, 1H, *J* = 1.8 Hz, *J* = 7.9 Hz), 8.04 (dd, 1H, *J*

= 1.8 Hz, $J = 8.0$ Hz), 7.37 (t, 1H, $J = 7.9$ Hz), 4.08 (s, 3H). ^{13}C NMR (75 MHz, CDCl_3): δ 164.98, 151.9, 144.5, 134.7, 127.3, 126.8, 122.8, 63.1. MS-ESI: calculated for $[\text{M}]^+$ ($\text{C}_8\text{H}_7\text{NO}_5$): m/z 197.0 found: m/z 197.2.

Methyl 2-methoxy-3-(2-methoxy-3-nitrobenzamido)benzoate (5): Acid **4** (3.00 g, 15.20 mmol) was dissolved in CH_2Cl_2 (30 ml) to which 4-methylmorpholine, NMM (2.2ml, 17.90 mmol) and ethyl chloroformate (1.9 ml, 16.40 mmol) was added at 0°C . The reaction mixture was stirred for at least 15 min then a solution of amine **3** (2.70 g, 14.90 mmol) dissolved in CH_2Cl_2 (30 ml) was added. The reaction mixture was allowed to stir continuously overnight at room temperature. The reaction mixture was washed with 1M KHSO_4 (100 ml), followed by saturated NaHCO_3 (100 ml) and saturated NaCl (100 ml). Drying over Na_2SO_4 and removal of solvent in *vacuo* gave the crude product, which was recrystallized from methanol to give the pure product **5** as a white solid. Yield: 3.49 g, 71%. ^1H NMR (300 MHz, CDCl_3): δ 10.37 (s, 1H), 8.80 (dd, 1H, $J = 1.6$ Hz, $J = 8.2$ Hz), 8.45 (dd, 1H, $J = 1.8$ Hz, $J = 7.9$ Hz), 8.00 (dd, 1H, $J = 1.8$ Hz, $J = 8.1$ Hz), 7.63 (dd, 1H, $J = 1.6$ Hz, $J = 7.9$), 7.44 (t, 1H, $J = 8.1$ Hz), 7.24 (t, 1H, $J = 8.1$), 4.10 (s, 3H), 3.95 (s, 6H). ^{13}C NMR (125 MHz, CDCl_3): δ 165.9, 161.3, 151.5, 149.4, 136.5, 132.7, 128.8, 126.6, 124.6, 123.5, 64.5, 62.6. MS-ESI: calculated for $[\text{M}]^+$ ($\text{C}_{17}\text{H}_{16}\text{N}_2\text{O}_7$): m/z 360.2, found: m/z 360.1.

3.2.3 Procedure for Demethylation:

Methyl 2-hydroxy-3-nitrobenzoate (1): Compound **2** (0.17 g, 1.00 mmol) was dissolved in solvent NMP (1 ml) and tetrabutylammonium halide salt (2.00 mmol) was added into the solution. The mixture was heated at 90°C for 2 hours. Then solvent was removed in *vacuo* and the residue was dissolved in CH₂Cl₂ and washed with water. Removal of CH₂Cl₂ gave a yellow solid which was purified by gradient flash column chromatography on silica gel (4 : 1 v/v hexane : EA) to give pure product as a bright yellow solid.

Methyl 3-(2-hydroxy-3-nitrobenzamido)-2-methoxybenzoate (6): Compound **5** (0.36 g, 1.00 mmol) was dissolved in NMP (1 ml) and tetrabutylammonium chloride (TBACl) (0.59 g, 2.00 mmol) was added into the solution. The mixture was heated at 90°C for 2 hours. The solvent was then removed in *vacuo* and the residue was dissolved in CH₂Cl₂ and washed with water. Removal of CH₂Cl₂ gave a yellow solid which was purified by gradient flash column chromatography on silica gel (4 : 1 v/v hexane : EA) to give pure product **6** as a bright yellow solid. ¹H NMR (300 MHz, CDCl₃): δ 12.38 (s, 1H), 10.53 (s, 1H), 8.80 (d, 1H, *J* = 8.2 Hz), 8.68 (d, 1H, *J* = 7.6 Hz), 8.38 (d, 1H, *J* = 8.2 Hz), 7.66 (d, 1H, *J* = 8.2 Hz), 7.22-7.27 (m, 2H), 3.99 (s, 3H), 3.97 (s, 3H). ¹³C NMR (125 MHz, CDCl₃): δ 165.9, 161.05, 152.97, 149.61, 140.79, 134.46, 132.93, 129.07, 126.51, 124.94, 124.39, 123.80, 120.45, 62.49, 52.33. MS-ESI: calculated for [M]⁺ (C₁₆H₁₄N₂O₇): *m/z* 347.3, found: *m/z* 347.2.

Methyl 2-hydroxy-3-(2-hydroxy-3-nitrobenzamido)benzoate (7): Compound **5** (0.36 g, 1.00 mmol) was dissolved in CH₃COOH (1 ml) and tetrabutylammonium chloride (TBACl) (0.59 g, 2.00 mmol) was added into the solution. The mixture was heated at 90°C for 2 hours. Then solvent was removed in *vacuo* and the residue was dissolved in CH₂Cl₂ and washed with water. Removal of CH₂Cl₂ gave a yellow solid which was purified by gradient flash column chromatography on silica gel (4 : 1 v/v hexane : EA) to give pure product **7** as a bright yellow solid. ¹H NMR (300 MHz, CDCl₃): δ 11.40 (s, 1H), 10.34 (s, 1H), 8.78 (d, 1H, *J* = 13.2 Hz), 8.63 (d, 1H, *J* = 12.9 Hz), 8.34 (d, 1H, *J* = 14.0 Hz), 7.63 (d, 1H, *J* = 13.4 Hz), 7.19 (t, 1H, *J* = 12.9 Hz), 6.97 (t, 1H, *J* = 13.4 Hz), 3.99 (s, 3H). ¹³C NMR (125 MHz, CDCl₃): δ 170.86, 161.18, 153.14, 151.17, 140.34, 134.55, 128.96, 127.50, 125.91, 124.40, 123.73, 120.19, 110.26, 111.89, 52.56. MS-ESI: calculated for [M]⁺ (C₁₅H₁₂N₂O₇): *m/z* 332.3, found: *m/z* 332.5.

3.3 Results and Discussion

3.3.1 Demethylation using TBACl

To find out the best demethylation reagent for aryl methyl ether cleavage, methyl 2-methoxy-3-nitrobenzoate **2** was subjected to treatment with various tetrabutylammonium salts (TBA salts) in the presence of 1-methyl-2-pyrrolidinone (NMP) at 90°C for 2 hours (**Table 3.1**). The reaction was found to be best carried out in dry NMP using either tetrabutylammonium bromide (TBABr) or

tetrabutylammonium chloride (TBACl) as the demethylation reagents. Other TBA salts such as tetrabutylammonium fluoride (TBAF) and tetrabutylammonium iodide (TBAI) gave the poor yields. The activity of TBAF probably was too high, causing many side reactions that led to a low chemical yield (35%). Additional demethylation experiments in NMP at 90°C for 2 hours were then performed on methyl 2-methoxy-3-(2-methoxy-3-nitrobenzamido)-benzoate **5** to compare the demethylation efficiency of TBACl with that of TBABr. The data presented in **Table 3.2** clearly proved TBACl (60% yield) to be superior than TBABr (<10% yield).

To explore the solvent effects on the demethylation reaction, methyl 2-methoxy-3-nitrobenzoate **2** was subjected to the treatment with TBACl under various solvents. As shown in **Table 3.3**, the originally used solvent NMP turned out to be the best solvent for the demethylation reaction promoted by TBACl. Reasonable yields were also obtained with other solvents such as DMSO (54%), toluene (66%) and HMPA (54%). When the reaction was carried out in NMP at 50°C for 4 hours, the chemical yield was significantly reduced compared to the reaction carried out at 90°C for 2 hours. It needs to be pointed out that the high reaction temperature (90°C) does not have any detrimental effects on either the product or the starting material.

Table 3.1. Effects of salts on the TBACl-mediated demethylation of compound **2**.

Entry	Salt	Solvent	Temp (°C)	Time (hrs)	Yield (%)
1	TBAF	NMP	90.0	2.0	35
2	TBACl	NMP	90.0	2.0	78
3	TBABr	NMP	90.0	2.0	73
4	TBAI	NMP	90.0	2.0	32

Table 3.2. Effects of salts on the TBACl-mediated demethylation of compound **5**.

Entry	Salt	Solvent	Temp (°C)	Time (hrs)	Yield (%)
1	TBACl	NMP	90.0	2.0	60
2	TBABr	NMP	90.0	2.0	<10

Table 3.3. Effects of solvents and temperatures on the TBACl-mediated demethylation of compound **2**.

Entry	Solvent	Temp (°C)	Time (h)	Yield (%)
1	NMP	50.0	4	25
2	NMP	90.0	2	78
3	CHCl ₃	60.0	2	30
4	CH ₃ COOH	90.0	2	35
5	DMF	90.0	2	29
6	DMSO	90.0	2	54
7	Acetonitrile	80.0	2	43
8	Toluene	90.0	2	66
9	HMPA	90.0	2	54

3.3.2 Demethylation of dimer

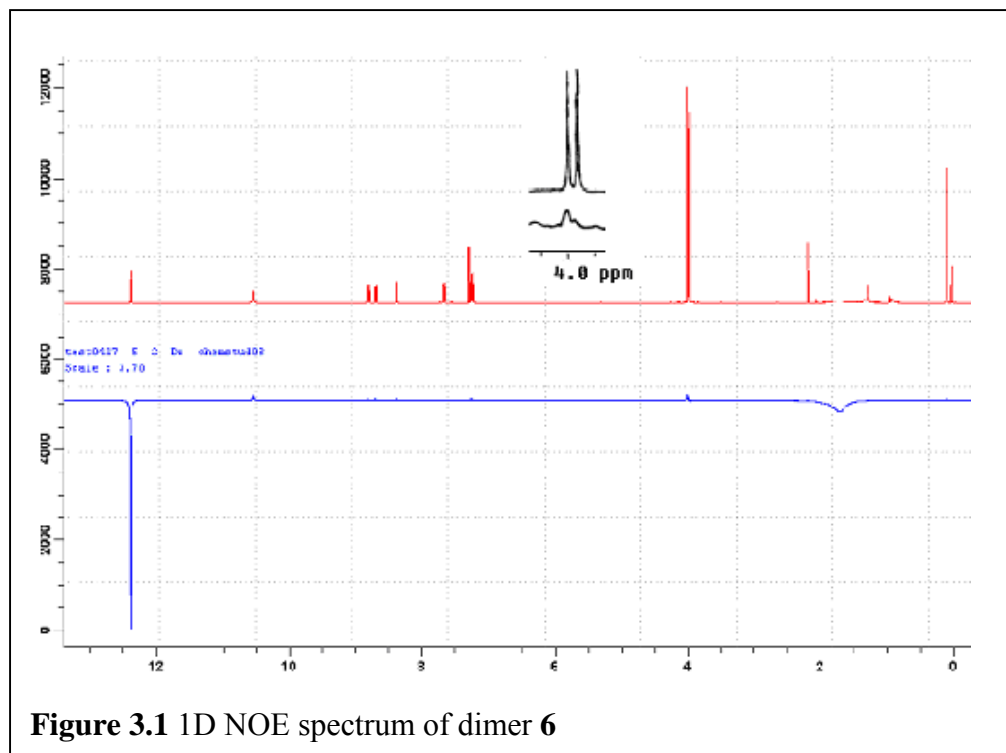
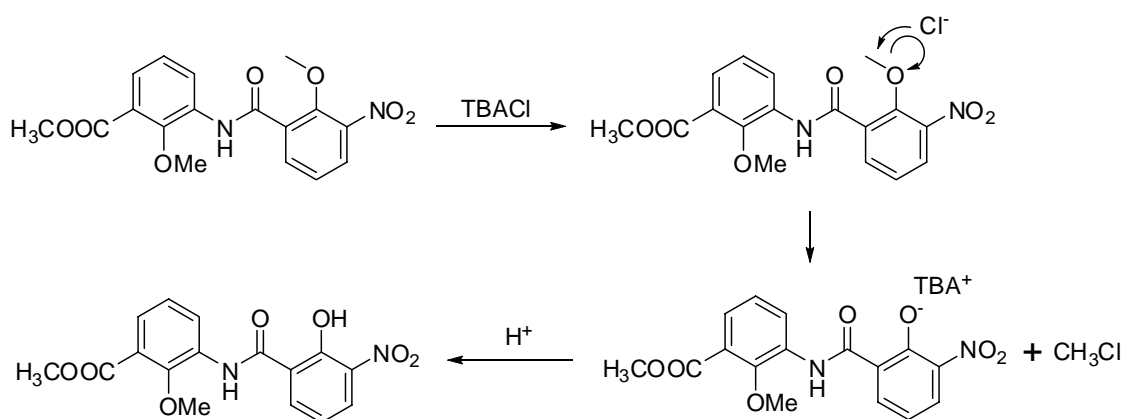


Figure 3.1 1D NOE spectrum of dimer **6**

As discussed above, the demethylation experiments were performed on dimer **5** in order to compare the demethylation efficiencies of TBACl and TBABr. Other purposes are (1) to test if the optimized conditions would work on the higher oligomers having more monomeric building blocks and (2) also to see if the reaction is selective or not. To our satisfaction, the TBACl-mediated demethylation reaction not only worked on the higher oligomers such as dimer **5**, but also led to the selective removal of methoxy methyl group immediately next to nitro group. The aryl methyl ether next to ester next to ester group remains intact (**Scheme 5**). This selective demethylation was confirmed by 1D NOE study (**Figure 3.1**) on **6**. From the 1D NOE spectrum obtained, when the phenol proton was irradiated, only one of the singlet peak with a proton integration of 3 protons shows a positive NOE signal, while the

other singlet is not being affected. This shows that the phenol is not located at the position between the methyl ester and the other methyl ether, but on the *ortho* position of the nitro group. Using other common organic solvent also gave the same product albeit with lower yields. These results led us to conclude (1) that the electron-withdrawing groups activate the aryl methyl ether linkage and make it more susceptible to the TBACl-mediated ether cleavage and (2) that TBACl can detect such a difference in electron density and selectively cleave the aryl methyl ether linkage next to the electron-withdrawing group. When acetic acid was used, it was observed that both the aryl methyl ether was removed, suggesting that the acid present in the reaction possibly protonates the methoxy oxygen atom, converting the methoxy methyl group into a better leaving group and so greatly facilitating the cleavage of ether linkages. The mechanism for the deprotection reaction by TBACl is proposed as follows:



Scheme 6. Possible mechanism for the TBACl-promoted demethylation as exemplified by dimer **5**

4. Conclusion

A new and effective methodology has been developed for the conversion of aryl methyl ether into its phenol moiety. The demethylation reaction involves the use of tetrabutylammonium chloride as the demethylation agent. The reaction is mild and may be used on molecules with sensitive functional groups. Different demethylation products can be obtained by using different solvents. In another word, when NMP is used as the solvent, only the aryl methyl ether next to an electron withdrawing group was demethylated. When acetic acid was used as the solvent, the less susceptible aryl methyl ether linkage was also cleaved under the same condition of heating at 90 °C for 2 hours. Further investigations on other molecules carrying electron withdrawing/donating groups of various types are still required to explore the usefulness and selectivity of this demethylation method.

References:

1. Chakraborti, A. K.; Sharma, L.; Nayak, M. K. *J. Org. Chem.* **2002**, 67, 6406.
2. Koutek, B.; Setinek, K. *Collect. Czech. Chem. Commun.* **1968**, 33, 866.
3. McCarthy J. R.; Moore, J. L.; Cregge, R. J. *Tetrahedron Lett.*, **1978**, 52, 5283.
4. Ohsawa, T.; Hatano, K.; Kayoh, K.; Kotabe, J.; Oishi, T. *Tetrahedron Lett.*, **1992**, 33, 5555.
5. Feutril, G. I.; Mirrington, R. N. *Tetrahedron Lett.* **1970**, 1327.

6. Sheehan, J. C.; Daves, Jr., G. D. *J. Org. Chem.* **1964**, 29, 2006.
 7. Nayak, M. K.; Chakraborti, A. K. *Tetrahedron Lett.*, **1997**, 38, 8749.
- Li, G.; Patel, D.; Hruby, V. J. *Tetrahedron Lett.*, **1993**, 34, 5393.

Chapter Four

Concluding Remarks

Synthetic ion channel has been an emerging field in supramolecular chemistry and in bioorganic chemistry. Synthetic ion channels have been synthesized by many groups and have found some interesting applications in such as catalysis and sensors.

In this thesis, pyridine-based crescent aromatic γ -peptides were designed, synthesized, characterized and analyzed. The introduction of some directional intramolecular hydrogen bonding interactions results in a number of backbone-rigidified oligomers, adopting a crescent conformation in solution and solid state. The experimental results obtained from these studies are in agreement with the theoretical calculations performed. The synthesized oligomers were tested for its binding affinities toward various anions, but results showed that there is essentially no binding between the oligomers and all the anions tested.

It is believed that incorporating one or two phenol-based building blocks into the oligomers would help to increase the binding ability toward the anions and even cations. Hence, a new methodology for converting the aryl methyl ether into the phenol derivatives was sought, developed and partially optimized. This new method involves the use of tetrabutylammonium chloride as the demethylation reagent.

Depending on the solvents used, this method can be quite selective and cleaves only the aryl methyl ether next to a nitro group.

By coupling the methoxy-based monomer to the pyridine based monomer, various mixed oligomers can be formed and the aryl methyl ether can then be cleaved using the new methodology disclosed herein to give the phenol derivatives.